



Norwegian University of
Science and Technology

Investigation of Inclusion Characteristics in LCAK Calcium Treated Steel

Inclusion characterization in 3-D using Electrolytic Extraction and
SEM

Rajat Sharma

Silicon and Ferroalloy Production

Submission date: November 2011

Supervisor: Ragnhild Aune, IMTE



KTH Industrial Engineering and Management

INVESTIGATION OF INCLUSION CHARACTERISTICS IN LCAK CALCIUM TREATED STEEL

Master Thesis

By

RAJAT SHARMA

Division of Applied Process Metallurgy

Department of Material Science and Engineering

Stockholm, Sweden July 2011

ACKNOWLEDGEMENTS

I would like to thank the Head of the department of Material Science and Engineering, Professor Pär Jönsson for providing me the opportunity to pursue my master thesis in Applied Process Metallurgy division KTH, Sweden.

I express my gratitude to the researcher and tutor of my thesis, Dr. Andrey Karasev for teaching me the skills and techniques useful for the project. His guidance and patience in solving my doubts and inspiring me to always achieve the best, contributes a large part in making this thesis a success.

I like to express my sincere thanks and gratitude to my supervisor Diana Vasiljevic whose tremendous interest and support throughout my project has proved to be the foundation of my work. Her discussions on important issues and constructive comments have greatly improved my analytical and writing skills. I am highly thankful to Diana and SSAB EMEA in Luleå for providing me the industrial samples for the study and guiding me to work efficiently.

I would also like to express my sincere gratitude to Professor Ragnhild Elizabeth Aune who has been a true inspiration and support throughout my master study program. I am highly thankful for her efforts and support in arranging my thesis project at KTH.

I thank Wen-Li Long for her technical instructions and guidance in SEM laboratory. I also thank Peter Åström for being considerate with my comfort in the process metallurgy division.

I would like to express my gratitude towards my friends Yanyan Bi, Liu Qiang and Megha Bhatnagar who shared technical and non-technical ideas and made my time a truly enjoyable one.

I express my deepest gratitude to my parents and sister who have always been with me and have kept me going through hard times. I am eternally thankful to the Almighty for making this endeavor a successful one.

ABSTRACT

The production of clean steel often involves elimination or modification of non-metallic inclusions into acceptable morphology and composition. Inclusions can be detrimental for the properties of the final steel product. The steel samples for the present study were received from SSAB EMEA steel plant in Luleå, Sweden. Four samples from single heat were taken during different stages of secondary refining. Inclusions were extracted from these by electrolytic extraction and collected on a film filter. The inclusions on the film filter were analyzed in SEM for size distribution, shape, morphology and chemical composition. The first part of the study deals with selection of appropriate electrolyte for electrolytic extraction of Ca treated steel samples. Second part of this study is based on the investigation of changes in the characteristics of inclusions with time during secondary refining of steel. Comparing 2% TEA and 10% AA electrolytes, 2% TEA was found to be more suitable for electrolytic extraction of Ca treated steel samples. It was found that during secondary refining, the number of inclusions per unit volume of steel first increase sharply upon Ca addition and then subsequently decrease. Ca treatment resulted in about 67-78 % of inclusions as liquid Ca aluminates which are beneficial for casting operation and are acceptable in the final cast product.

Table of Contents

1. INTRODUCTION	5
2. LITERATURE REVIEW	6
2.1 Secondary refining of Steel	6
2.1.1 <i>Stages in secondary refining of steel</i>	6
2.1.2 <i>CAS-OB process</i>	8
2.1.3 <i>Deoxidation</i>	9
2.1.4 <i>Ca treatment</i>	10
2.1.5 <i>Steel sampling</i>	15
2.2 Inclusion Engineering	16
2.2.1 <i>Inclusion formation</i>	16
2.2.2 <i>Nucleation and growth of inclusions</i>	17
2.2.3 <i>Effects on steel properties</i>	17
2.2.4 <i>Methods of characterization of inclusions</i>	18
2.3 Instruments and methods	19
2.3.1 <i>Electrolysis principles</i>	19
2.3.2 <i>SEM and EDS</i>	20
3. EXPERIMENTS	20
3.1 Sample preparation	20
3.2 Electrolytic Extraction (EE)	21
3.3 SEM observation	25
4. RESULTS AND DISCUSSION	26
4.1 Selection of electrolyte for electrolytic extraction	26
4.1.1 <i>Particle size distribution</i>	27
4.1.2 <i>Shape and morphology comparison</i>	29
4.1.3 <i>Chemical composition of inclusions</i>	32
4.2 Changes in inclusion characteristics during secondary refining	36
4.2.1 <i>Particle size distribution</i>	36
4.2.2 <i>Morphology</i>	39
4.2.3 <i>Chemical composition of inclusions</i>	41
5. CONCLUSIONS	47
6. FUTURE WORK	48
7. REFERENCES	49

1. INTRODUCTION

In the production of Al-killed steels, alumina inclusions degrade the mechanical properties of the steel product. Ca treatment is a common practice for modification of solid alumina inclusions into liquid Ca aluminates. These modifications are required to avoid problems like nozzle clogging during continuous casting and these inclusions are also more acceptable in the final product.

There are several methods to study the characteristics of these inclusions. These methods can be classified into two main categories, 2D methods of observing the cross section of the sample for inclusions and 3D methods which involve the volumetric analysis of the whole inclusion. 3D methods provide more reliable information regarding inclusion characteristics such as the number of inclusions. It also gives the information about real shape and morphology of the inclusions.

The LCAK Ca treated steel samples for the present study were received from SSAB EMEA steel plant in Luleå, Sweden. The first part of the present study deals with the selection of an appropriate electrolyte for the electrolytic extraction of Ca treated steel samples. This was a necessary and an important part of the work since three out of four steel samples were Ca treated. This selection was aimed to select the electrolyte which preserves the original properties of inclusions for SEM analysis. In this way, the analysis results could reflect the true picture of inclusions in the steel. The second part of this work was aimed to investigate the changes in the inclusion characteristics as a function of time and see the effect of each stage of steel refining on the non-metallic inclusions. The results obtained from this study will help in attaining a better understanding of the transformation of inclusions during different stages of secondary refining of steel.

2. LITERATURE REVIEW

2.1 Secondary refining of Steel

2.1.1 Stages in secondary refining of steel

Steel is generally produced by two main routes, namely the ore based and scrap based route. Both cases require secondary refining of steel in order to reduce tap-to-tap time in the converter or electric arc furnace (EAF), and also to adjust the composition and temperature of liquid steel to desired level before casting. A schematic illustration of the general steps in secondary steelmaking is shown in Figure 1.

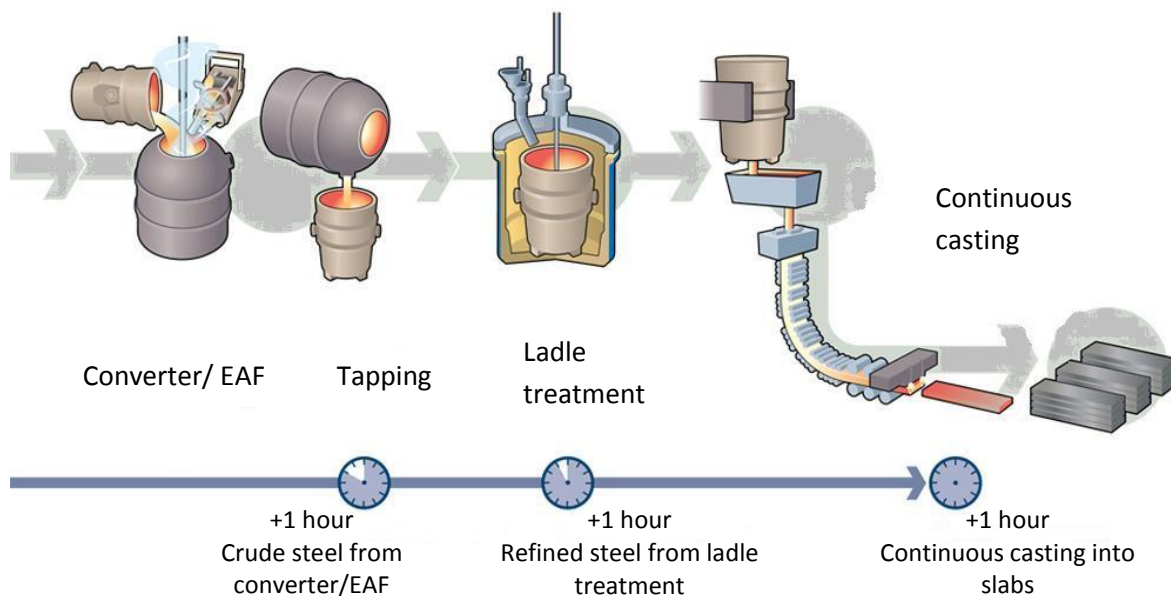


Figure 1: Steps in secondary steelmaking¹

When raw steel is tapped from the converter/EAF to the ladle, it contains some carry over slag. This slag is high in FeO - MnO content and can result in low yield of deoxidizing and alloying elements. Thus, it is replaced with CaO - Al₂O₃ based synthetic slag^{2,3}. Top slag serves the purpose of removing sulfur and non-metallic inclusions from the melt, protecting the liquid steel from surrounding atmosphere, and providing heat insulation^{2,4}. Deoxidizing elements like aluminium are added to the ladle for deoxidation of the melt. Dissolved

oxygen in the steel reacts with aluminium very quickly to form alumina inclusions. The ladle is subsequently transferred to a treatment station where some alloying elements are added, mostly in the form of ferroalloys or cored wires. Stirring of the liquid steel is practiced to achieve homogeneity both in terms of temperature and composition. Three types of stirring, namely, gas, induction and mechanical stirring can be used in industrial setup. Out of these, gas stirring is most commonly employed as it requires least investment and gives fairly good results. If required, temperature of liquid steel can be increased by graphite electrode heating or chemical heating (e.g. by addition of Al and O₂) to desired level which will ensure smooth casting operation. If the temperature of the melt is too high, it can be reduced by adding scrap metal^{2,5}.

After alloying and temperature adjustment of the melt, the ladle is transferred to the continuous casting station where the liquid steel from the ladle is poured into the tundish through a nozzle. The liquid steel from the tundish is then allowed to pass through a nozzle into the mold and cooled by streams of water to carry out the continuous casting operation. Another form of casting called ingot casting is used in small scale casting operations and is less productive than continuous casting.

In the present study, low-carbon⁶ aluminium-killed (LCAK) steel samples with carbon content of 0.15 wt% were received from SSAB EMEA steel plant located in Luleå, Sweden. It is an ore-based steel plant which has a coking plant, one operating blast furnace, hot metal desulphurization in open ladles, two 130 tons BOF-LBE converters, two CAS-OB stations, RH degasser and two slab casters⁵. Ca treatment is employed to modify the inclusions in the liquid steel and Ar gas bubbling is utilized for stirring and protection from the atmosphere while alloying. In LCAK steel due to low carbon content, the amount of dissolved oxygen is expected to be high after the converter process. This results in the formation of large number of non-metallic inclusions of different characteristics. The samples used in the present study were from a single heat of secondary refining through a CAS-OB route.

2.1.2 CAS-OB process

CAS-OB stands for 'Composition Adjustment by Sealed argon bubbling-Oxygen Blowing'. It is a steel treatment process during secondary refining to alloy and heat the steel to the required temperature prior to casting. These fine adjustments are very crucial in order to obtain the required chemical composition of the final cast product and avoid any defects. A schematic illustration of the CAS-OB station is presented in Figure 2.

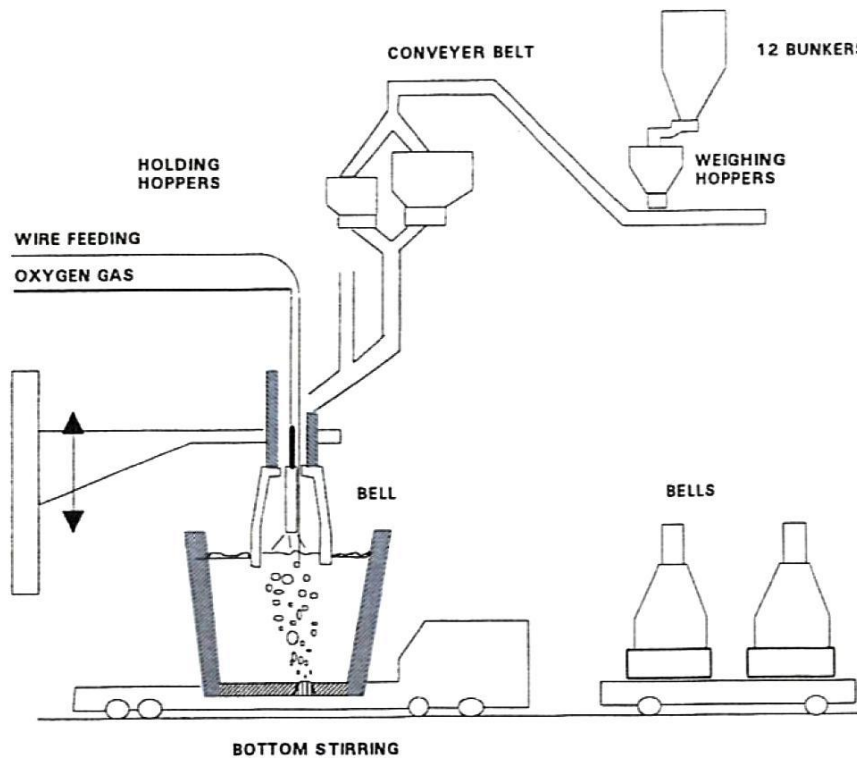


Figure 2: Schematic illustration of CAS-OB process⁵

At the CAS-OB station, the Ar gas flow, introduced through a porous plug centered at the bottom of the ladle, is adjusted such that an open eye is formed on the melt surface. This open eye removes the slag from a portion of the top surface so that a bell arm can be lowered and alloying elements can be injected into the steel melt. The inert Ar atmosphere leads to high yield of these added alloys². By adding controlled amount of Al granules and O₂, the steel can be chemically heated to the desired temperature. During this treatment, the gas injection also leads to stirring of the melt to remove the resultant deoxidation products and homogenize the chemical composition and temperature. After the treatment at the CAS-OB station, the liquid steel in the ladle is transferred to the continuous casting

station. The treatment time at the CAS-OB station in SSAB Luleå works, Sweden is on average 28 minutes⁵.

2.1.3 Deoxidation

Raw steel obtained from the converter contains dissolved oxygen of the order of 200-1000 ppm^{2,7}. If not decreased, this high oxygen content will result in low yield of alloying additions. Due to decreasing solubility during solidification, the rejected oxygen may react with carbon and alloying elements present in the steel to form CO and non-metallic inclusions, respectively². Formation of gases like CO leads to problems like blowholes and pinholes while the oxide formation results in surface or sub-surface porosity which is detrimental for the properties of final product⁸.

When deoxidizers like Al and Si are added to the steel melt, large number of primary inclusions nucleates in a very short time. The dissolved oxygen content of steel is expected to reduce to equilibrium value. This behavior is shown in Figure 3. The total oxygen content is the sum of dissolved oxygen and oxide inclusions. Stirring promotes growth and removal of inclusions and this practice is called precipitation deoxidation².

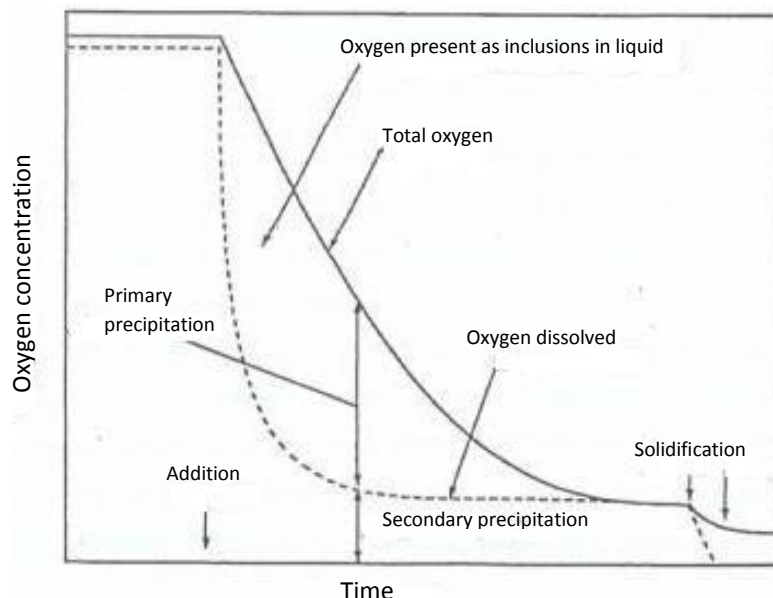


Figure 3: Schematic diagram of oxygen decrease during deoxidation⁹

Sometimes complex deoxidation is also used to achieve even lower oxygen content in the final product. It requires formation of complex inclusions composed of several different oxides. The advantage here is that the deoxidation product is more stable and its activity is reduced due to its dissolution in several other oxides^{2,10}.

2.1.4 Ca treatment

Modification of alumina inclusions in steel melt by Ca treatment is common practice employed prior to continuous casting of low carbon steel. Alumina inclusions formed after aluminium addition are solid particles and tend to form clusters. This cluster formation can lead to blockage of the submerged entry nozzle (SEN) during casting (Figure 4) which can disrupt the entire casting operation¹¹.

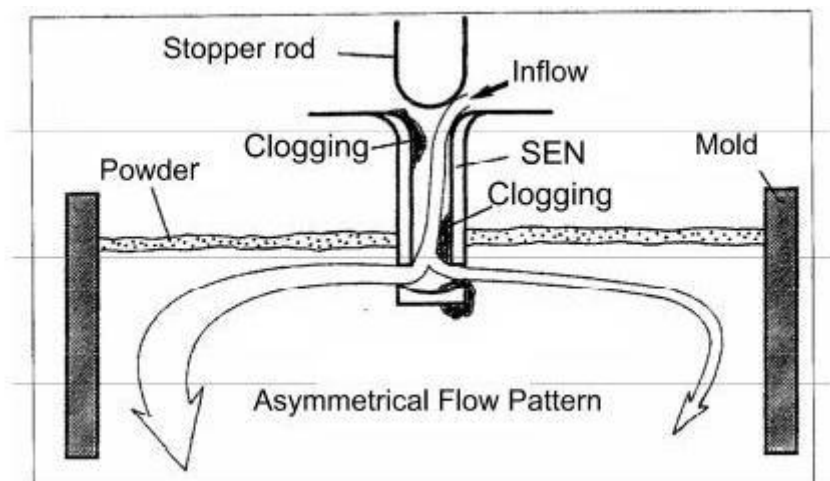


Figure 4: Submerged Entry Nozzle (SEN) clogging¹²

Addition of Ca (e.g. as CaSi wire feed) improves the castability of the steel as shown in Figure 5. Ca treatment leads to the formation of Ca aluminates which are liquid at molten steel temperature and do not form clusters, thereby preventing the nozzle from blocking up^{2,13,14,15,16}. Flow factor (castability), which is a ratio of actual casting speed to theoretical casting speed for a given nozzle size and tundish depth, has been found to decrease when the sulphur content increases¹⁷. Addition of Ca reduces the dissolved oxygen content of

liquid steel and enlarges the existing field of liquid phases. Thus, more Al can be added maintaining the liquid inclusions, thus favoring the floatation of inclusions and casting¹³.

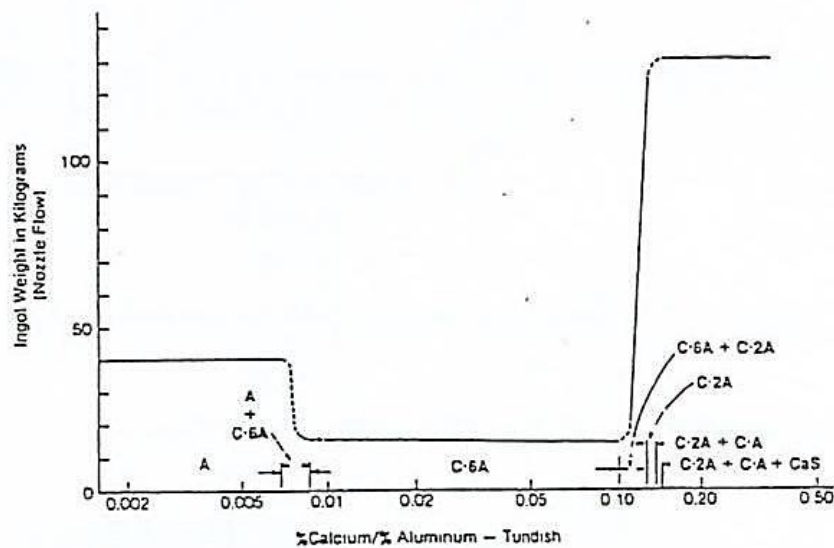


Figure 5: Influence of Ca/Al ratio on castability of Al killed steel¹⁷

Liquid phase is considered to have a lower density compared to the solid phase. Thus, liquid Ca aluminates are expected to be easy to separate from the molten metal as they float to the surface during stirring. They may also coalesce together to form larger droplets which will lead to more buoyant force helping their floatation and separation at the metal-slag interface⁷. In contrast, another study suggests that Ca aluminates do not have tendency to coalesce even in liquid state which decreases their chances of separating to slag phase¹⁸. A predominant factor in determining the rate of separation of inclusions into metal-slag interface is the wettability of the inclusion. The adhesion work which determines the wettability of the inclusion is given by:¹⁹

$$W_A = \lambda_M (1 + \cos \theta) \quad (0)$$

Here λ_M is the surface tension of liquid steel and θ is the contact angle. It shows that the larger contact angle, the lesser is the work of adhesion which implies less energy required for its separation. Since the contact angle of spherical liquid inclusions is much lower than non-spherical inclusions, their separation from the melt will take more time and energy¹⁹.

Figure 6 shows the binary phase diagram of a CaO-Al₂O₃ system. It clearly shows that in order to form liquid Ca aluminates at the steel melt temperature (about 1500°C) the amount of Ca added to the steel melt must fall within a certain desirable range close to 50 wt% CaO.

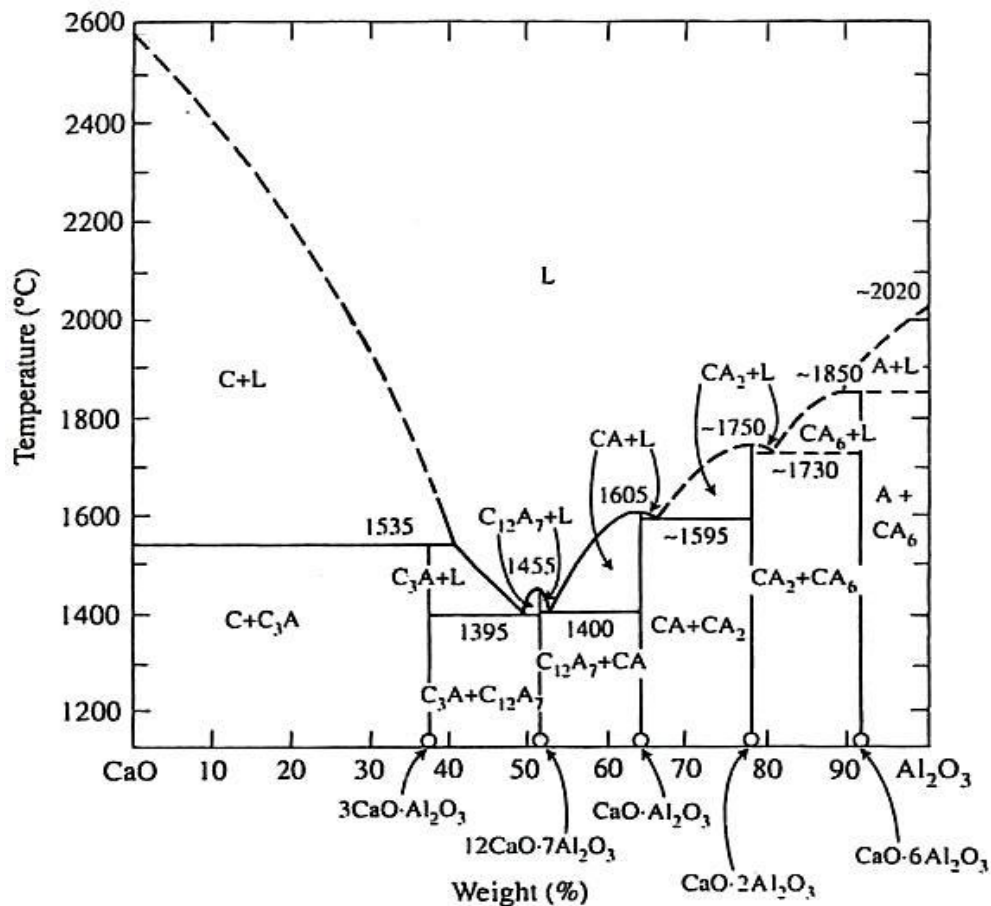


Figure 6: Binary phase diagram of CaO-Al₂O₃ system²⁰

The binary phase diagram shows that the melting point of Ca aluminate decreases as CaO content increases up to a certain limit. Eutectic temperature of CaO-Al₂O₃ system has been reported to be 1395°C at about 53% Al₂O₃²¹. Modification of alumina inclusions is achieved only for CaO content in the range 25-60 %²².

When Ca is added to liquid steel, it can react according to any of the reactions given below:





From reaction (2),

$$\frac{a_{Ca}^3 \cdot K}{a_{Al}^2} = \frac{a_{CaO}^3}{a_{Al_2O_3}} \quad (0)$$

Equation (5) shows that for about 50% CaO in binary CaO-Al₂O₃ system, the amount of Ca which should be added can be estimated by activities of CaO and Al₂O₃ using Figure 7.

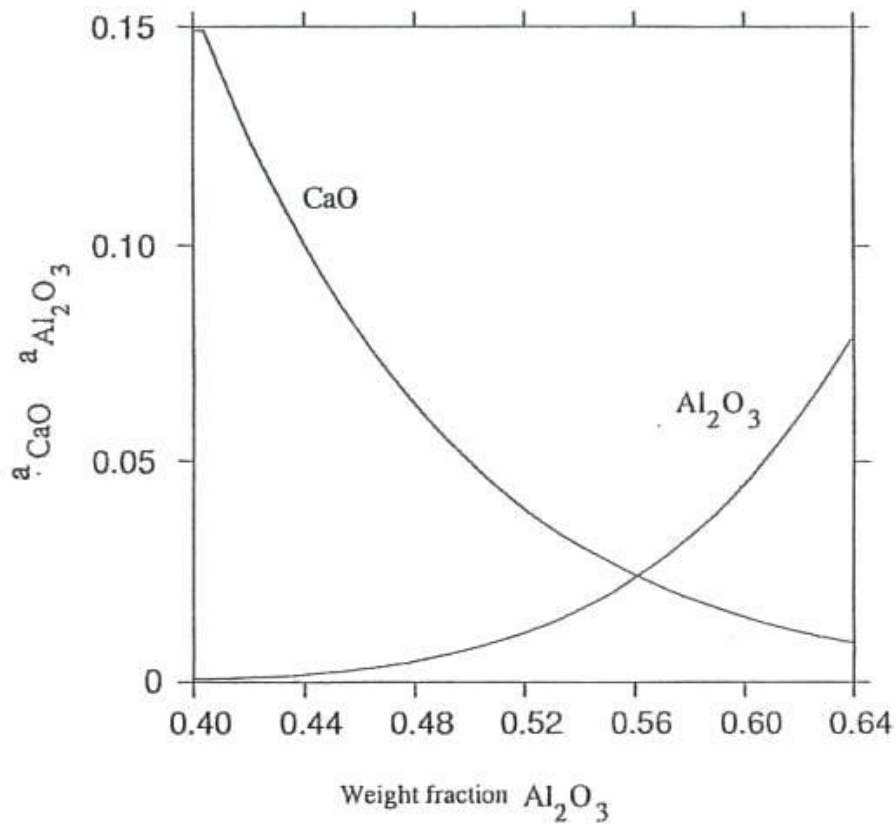
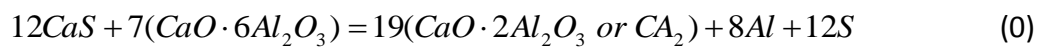
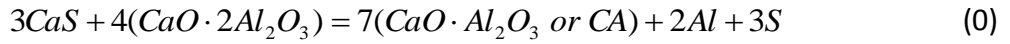


Figure 7: Activity of CaO and Al₂O₃ as a function of composition of liquid Ca aluminate at 1500 °C²¹

The formation of various phases can be represented by following equations:²³





According to Pires and Garcia¹³, Ca has higher affinity for oxygen than S.²⁴ Hence, it initially converts alumina inclusions into solid Ca aluminates. If the S content of the melt is high, Ca will start forming sulphides until the S content of the melt is lowered. Then it will again start converting Ca aluminates to liquid phases. Figure 8 shows the variation of wt% S with wt% Al at two different temperatures. In a melt containing S above $C_{12}A_7$ curve, added Ca will first convert alumina inclusions into CA. More addition of Ca will result in formation of CaS until the amount of S is lowered below $C_{12}A_7$ line. Ca added after this stage will react with CA to convert it into liquid $C_{12}A_7$ aluminates. Steel must be desulphurized to low levels (less than 40 ppm) before Ca treatment to prevent the precipitation of CaS^{11,25}. Formation of CaS is avoided because they can contribute to the same problem of nozzle clogging as the alumina inclusions since they are solid particles at casting temperature.

Concentration of S in equilibrium with Ca aluminates decreases during solidification and excess S is precipitated in the form of CaS shells surrounding the aluminates^{13,22,26}. The amount of CaS will depend on Mn content of steel; the higher the Mn content, the lower is the activity of CaS¹³. By optimum Ca treatment, the S is bound to the oxide or aluminate particles and is not deposited as sulphide inclusions at grain boundaries during steel solidification^{27,28}. Formation of Ca aluminates having about 50 wt% CaO and not having a sulphide shell is possible with S content less than 40 ppm²⁹.

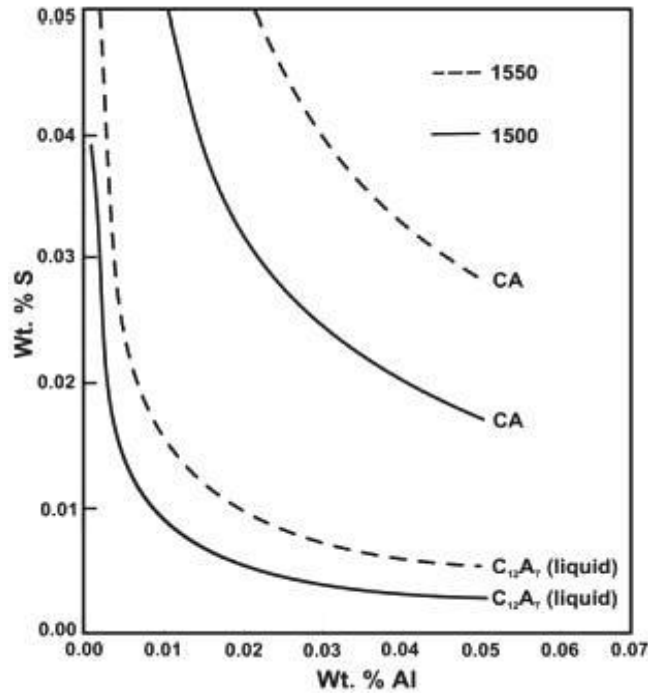


Figure 8: Invariant equilibrium for CaS and $C_{12}A_7$ or CA as a function of wt% Al and S at two temperatures ($^{\circ}C$)³⁰

2.1.5 Steel sampling

The dual thickness lollipop samples were received from SSAB EMEA steel plant in Luleå, Sweden. Ca addition is practiced at SSAB, Luleå to modify the composition of inclusions from solid alumina to liquid Ca aluminates. Samples were taken manually from different stages of a single heat of ladle refining process using an Ar protected sampler. Ar gas creates a small slag-free area on the melt surface to introduce the sampler. Two samples were taken from the ladle at the CAS-OB station; one before (S1) and one just after (S2) the Ca addition. Two additional samples were taken from the tundish at the continuous casting station, one at 20 minutes after the start (S3) and the other at the end (S4) of continuous casting. PDA-OES analysis was conducted on the samples by SSAB before they were received for experiments in the present study. The points where PDA-OES analysis was already performed can be seen as white spots on the sample surface in Figure 9.



(a)

(b)

Figure 9: (a) Front view and (b) side view of prototype of dual thickness lollipop steel samples received from SSAB steel plant in Luleå, Sweden

2.2 Inclusion Engineering

2.2.1 Inclusion formation

Most common types of non-metallic inclusions are oxides, sulphides, oxysulphides, nitrides and carbonitrides²¹. Oxides form a large proportion of non-metallic inclusions due to high oxygen content in liquid steel after the converter process. To reduce the content of dissolved oxygen, certain deoxidizing agents like Al or Si are added to the steel bath which due to high oxygen affinity, form oxides. Typical oxide inclusions like alumina and silica are sometimes modified by Ca treatment to prevent casting problems.

Inclusions are generally classified as indigenous or exogenous, based on their source of formation. Primary indigenous inclusions include metal oxides formed as a result of deoxidation of liquid steel. Secondary inclusions precipitate when the solubility of dissolved oxygen decreases due to decrease in temperature during solidification. Exogenous inclusions are formed as a result of reoxidation of steel melt, slag entrainment and erosion of refractory lining.

2.2.2 Nucleation and growth of inclusions

After initial addition of deoxidizing agent to liquid steel, inclusions nucleate quickly. This stage is controlled by diffusion of deoxidizing agent and oxygen^{31,32,33}. Ostwald ripening occurs when the larger inclusions grow at the cost of smaller particles. This happens because of different surface tension and oxygen concentration gradients near particles of different sizes. Brownian motion is another cause of collision between particles resulting in their growth³³. Once the particles achieve a considerable size, turbulent collisions and Stokes collision become dominating mechanisms to promote their continued growth.³⁴ Density difference between liquid steel and inclusions, along with bubble attachment and convective fluid transport, causes removal of larger inclusions³⁵.

Alumina inclusions have been observed to form 3 dimensional clusters via collision and aggregation due to high interfacial energy¹². The clusters of dendritic alumina are found to be in the size range 30 to 100 μm , while coral shaped alumina inclusions are found to be smaller than 50 μm ³⁶. Spherical deoxidation inclusions are smaller and exist as single phase¹². Spherical exogenous inclusions are generally larger ($>50\mu\text{m}$), multiphase and frequently act as nucleus for the growth of indigenous inclusions¹².

2.2.3 Effects on steel properties

Inclusions are one of the main reasons for poor properties of the final steel product. In some cases, the degradation can be seen visually in form of poor surface finish. It becomes more crucial when it comes to mechanical properties like ductility, fracture toughness and resistance to corrosion as these are not detected visually but can lead to more dangerous consequences²⁸. These inclusions or precipitates act as stress raisers as they hinder the dislocation movement, thus causing hardening of the material^{37,38,39}.

Some inclusions may also have a positive effect on steel matrix. Oxide inclusions act as nucleation sites for acicular ferrite during the austenite to ferrite phase transformation, mostly in low carbon steels⁶. This improves the metal bond during welding⁴⁰. Oxide inclusions act as trapping sites for hydrogen atoms in enameled steel, thus preventing the coating film from stripping off⁴⁰. Sulphide inclusions are also expected to improve the machinability of free-cutting steels⁴⁰.

2.2.4 Methods of characterization of inclusions

Methods to characterize inclusions can be generally classified into two types:

- Two dimensional (2D) method which involves observation of inclusions on the cross section of the sample
- Three dimensional (3D) methods which involves volumetric analysis of inclusions

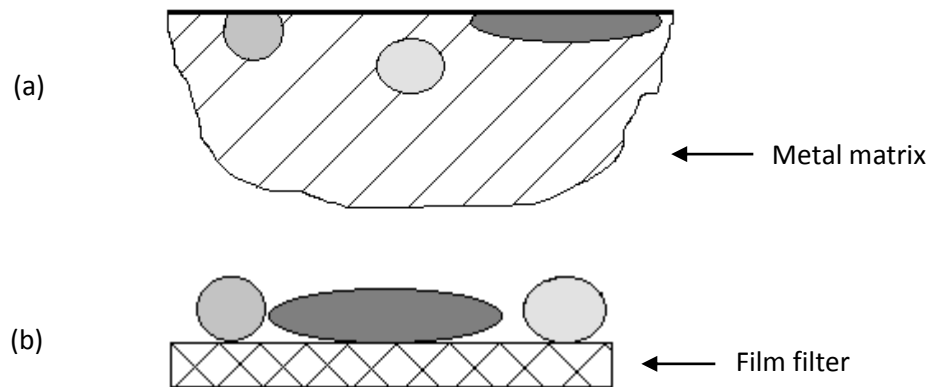


Figure 10: (a) 2D method and (b) 3D electrolytic extraction method

2D method gives the advantage of knowing the exact position of inclusions on the sample cross section. It also gives an estimate about the original morphology of inclusions in steel e.g. if the original inclusions consist of several phases or have holes. This original morphology can be affected to some extent with the 3D method. In the electrolytic extraction, if the electrolyte preferentially dissolves some phase, it becomes difficult to decide if the electrolyte created the holes or they were present in the original inclusions. However, the 3D method has some advantages over the 2D method as it gives a true picture of the size of inclusions and not only the inclusion's cross-section. Since the 3D method investigates the inclusions from a volume of the sample, the probability of finding inclusions of all size range is higher than that of the observation of the sample's cross section.

Extraction of inclusions for 3D analysis can be done either by electrolytic extraction or chemical dissolution of steel matrix in acid like HCl. It has been proved that for Ca aluminate inclusions, which are the subject of the present study, acid dissolution is inappropriate and electrolytic extraction is a better method⁴. In electrolytic extraction method, the chemical

analysis of inclusions by using SEM-EDS is more reliable as it is not affected by other elements present in the steel matrix. However, it can be affected to some extent by carbon present in the film filter^{18,41}. Other 3D methods used for inclusion characterization include sulphur print and Pulse Distribution Analysis Optical Emission Spectrometry (PDA-OES)¹⁸.

2.3 Instruments and methods

2.3.1 Electrolysis principles

Electrolytic cell used in the present study works on the principle of electric charge transfer by ions through the electrolyte to complete the electrical circuit. The applied voltage creates potential difference between the electrodes which generates an electric field for the movement of charge. The schematic diagram of electrolytic cell is shown in Figure 11. In the present experiments, the sample was made anode so that it gets dissolved on the surface. In this way, the inclusions being non-conductive were settled down in the solution as anode mud. Later this solution was filtered to collect the inclusions on a film filter for analysis using SEM.

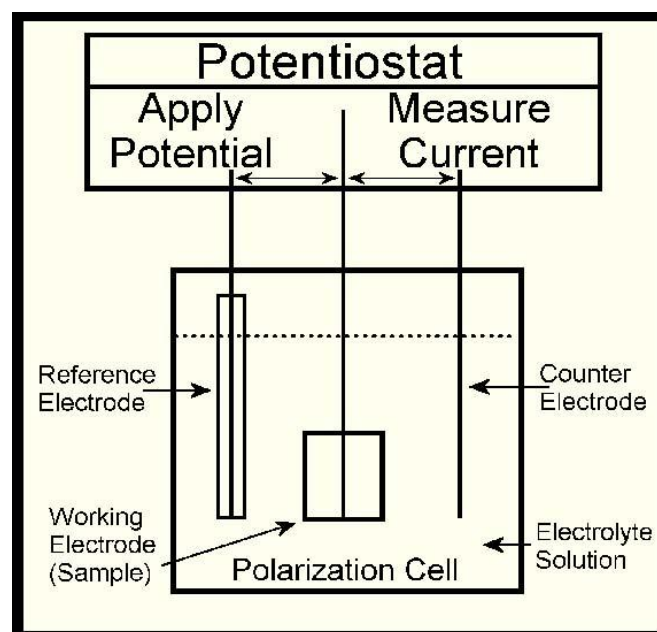


Figure 11: Electrolytic cell⁴²

2.3.2 SEM and EDS

Scanning Electron Microscope (SEM) is used for the observation of microstructures at magnifications much higher than optical microscope. It uses an electron beam which scans over the surface of the specimen and a detector receives signals to generate the image. Energy Dispersive X-ray Spectroscopy (EDS) is an analytical method used for the chemical characterization of the specimen. It is integrated with the SEM setup. It provides the elemental mapping of the specimen by using X-rays, thus, providing spectrum of all the elements present at the point or area of analysis. This function is based on the principle that all elements have a characteristic X-ray with a unique energy value. These different X-rays are collected by the detector which produces the spectrum of elements.

3. Experiments

3.1 Sample preparation

In the present study, the dual thickness lollipop samples were cut into desired dimensions of about 20*10*3 mm as shown in Figure 12. These sample dimensions were suitable for the EE setup used in the present study.

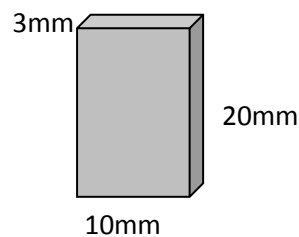


Figure 12: Schematic illustration of metal sample dimensions

The sample surfaces were ground in order to eliminate the top oxide layer. The sample was cleaned in two steps, first with acetone followed by cleaning with benzene, using an ultrasonic vibrator bath. Finally, the sample was dried and initial weight and dimensions were recorded prior to extraction. The surface having the PDA marks was chosen for electrolytic dissolution so that the results of present study can be confirmed with those of

PDA analysis. It should, however, be noted that PDA analysis is out of scope of the present study which deals only with EE method and inclusion characteristics evaluation using SEM. Since only one surface of the sample was of interest for dissolution, a thin paraffin film was applied to the other surfaces.

3.2 Electrolytic Extraction (EE)

The schematic representation of EE and filtration setup used in the present study can be seen in Figure 13. The sample is made anode and platinum wire is used as a reference electrode.

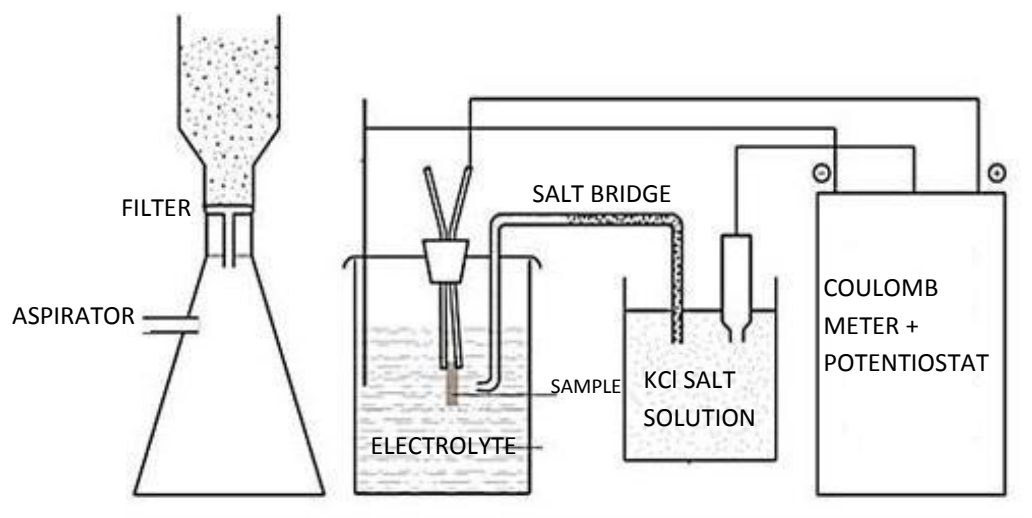


Figure 13: Schematic EE and filtration setup⁴³

In EE, the steel sample was dissolved on the surface by using electric current. During the extraction experiment, the charge and current were noted at regular intervals of 15-30 min. Target charge was fixed at 500 C in all cases. The non-metallic inclusions were extracted out from the steel matrix and collected on a thin film filter after filtration.

The main steps of EE in the present work are as follows:

1. The sample preparation is done according to the procedure explained in section 3.1.
2. Before setting up the experiment, the EE apparatus was cleaned first with plain water followed by distilled water and finally with methanol. Each step was repeated

three times to ensure desired level of cleanliness. This was done to make sure that the external particles like dust may not enter the system and block the free observation of the undissolved inclusions.

3. A beaker was filled with 250 ml of electrolyte and the sample was attached to the platinum clamp which was connected to the positive terminal of the potentiostat.
4. A coulomb meter attached to the potentiostat was used to regulate the amount of charge supplied to the system.
5. A platinum wire was immersed in the electrolyte which was used as a reference electrode.
6. EE is started when the potentiostat was turned on and current was allowed to pass through the system. It stopped after reaching the target charge.
7. In the filtration setup, the electrolyte was allowed to pass through a polycarbonate film filter with an open pore size of 0.05 μm . The undissolved particles were collected on the film filter which was thereafter analyzed in SEM.

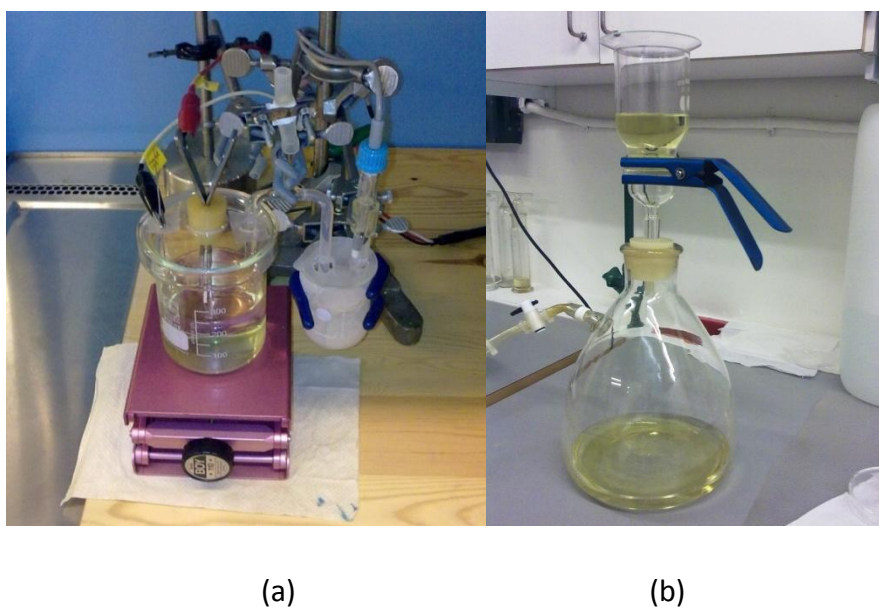


Figure 14: (a) EE experiment and (b) Filtration process

Steel samples were taken from different stages of single heat of secondary refining. Due to alloying and Ca addition at CAS-OB station, it was expected that these samples differ in

inclusion composition regarding Ca and Al content. Due to this difference in composition, it was necessary to first select a suitable electrolyte for the present work. A suitable electrolyte would allow the dissolution of the metal during EE but preserve the shape, size, composition and morphology of non-metallic inclusions present in the sample.

The two electrolytes which were investigated in the present study of inclusions were:

- 10% AA (10% acetylacetone - 1% tetramethylammonium chloride - methanol)
- 2% TEA (2% triethanolamine- 1% tetramethylammonium chloride- methanol)

For comparison of these two electrolytes, it was decided to observe the effect of these electrolytes on the inclusions by performing EE on sample S4 taken at the end of the continuous casting process. This selection results have been discussed in section 4.1.

After the selection of an appropriate electrolyte, EE was performed on the other samples and similar procedure was adopted to analyze the inclusions present in each sample. The rate of increase of charge for different samples has been plotted in Figure 15.

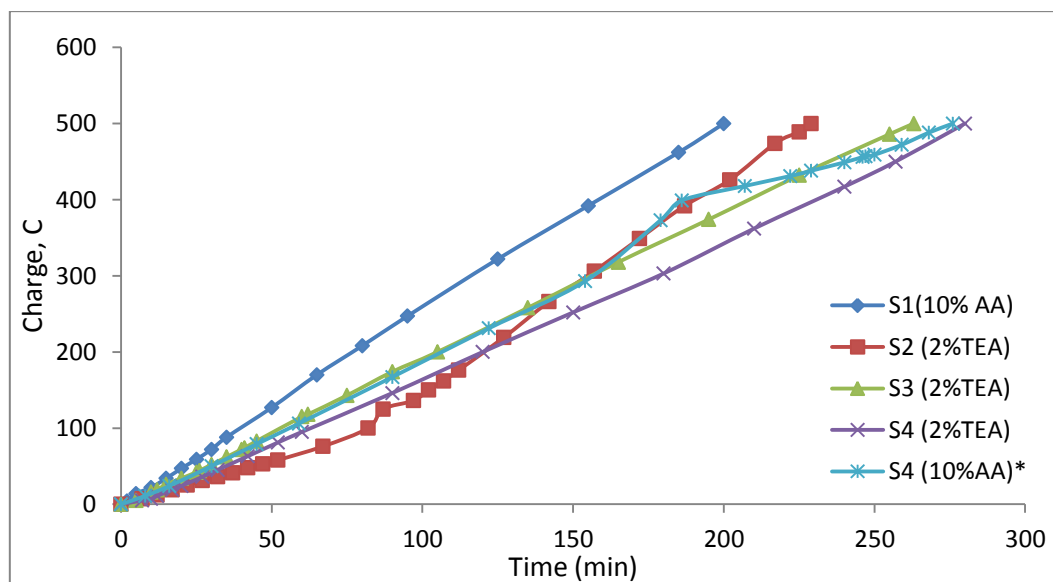


Figure 15: Increase in charge with time during five EE experiments

*Only for selection of electrolyte

Almost same slope for all five experiments ensures that the rate of dissolution was similar in all cases. Hence, the risk of inclusion characteristics being affected due to extraction conditions was minimized. EE experimental data for the different samples are presented in Table 1. The density value (ρ) of 0.0078 g/mm³ is used for all LCAK steel samples.

The dissolved thickness is calculated by using the formula:

$$\Delta t = \frac{\Delta m}{L \cdot B \cdot \rho} \quad (0)$$

Table 1: EE data of different steel samples

Sample	S1	S2	S3	S4	S4*
Electrolyte used	10% AA	2%TEA	2% TEA	2% TEA	10%AA
Sample dimensions LxB (mm)	15.52x14.94	17.8x13.55	21.23x13.4	17.8x9.71	18.04x9.95
Dissolved thickness $\Delta t(\mu\text{m})$	81	73	64	100	99
Dissolved weight Δm (g)	0.1418	0.138	0.1422	0.136	0.1393
Current(mA)	40	45	30	30	25
Voltage(V)	5	5	5	20	10
Time(min)	200	229	263	280	276
Slope	2.5288	2.2500	1.9293	1.7860	1.8828
R ²	0.9994	0.9757	0.9998	0.9993	0.9923

*Only for selection of electrolyte

3.3 SEM observation

SEM model S-3700N HITACHI was used to analyze the number, size and morphology of the inclusions. Chemical composition was analyzed using SEM-EDS. For SEM analysis, the film filter was cut into conical shape and assigned three zones as shown in Figure 16.

The analysis of particles in different zones is vital to ensure that wide range of particles are covered which leads to more reliable results.

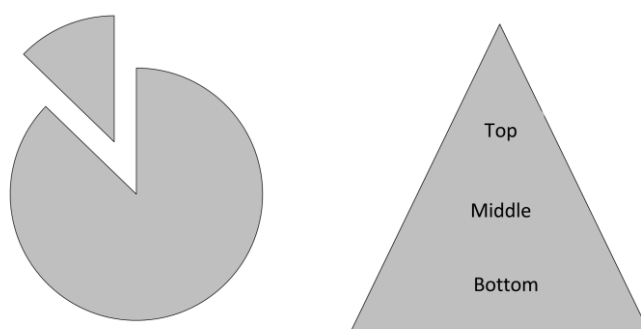


Figure 16: Film filter divided into three zones

All the film filters were analyzed in SEM using Scanning Electron imaging (SE) to evaluate the shape, size and morphology of inclusions. Inclusion composition was analyzed in Back Scattered Electron imaging (BSE) mode using Energy Dispersive X-ray Spectroscopy (EDS) with 100 s of live time per inclusion. The amounts of Al, Ca, S, O and Mg were quantified. At least 40 inclusions (20 each at top and bottom of filter) were analyzed per film filter for composition. At least 100 inclusions per film filter were analyzed for morphology of inclusions. Inclusion morphology is assessed by observing the inclusions for dissolved phases or holes. About 0.34 mm² area on the film filter was analyzed for particle size distribution.

Micrographs at magnification x1000 for S1, S3 and S4 and x3000 for S2 were taken for areas in top and bottom zones. A higher magnification was used for S2 as the inclusions were much smaller and difficult to quantify at x1000. Typical SEM micrograph is shown in Figure 17.

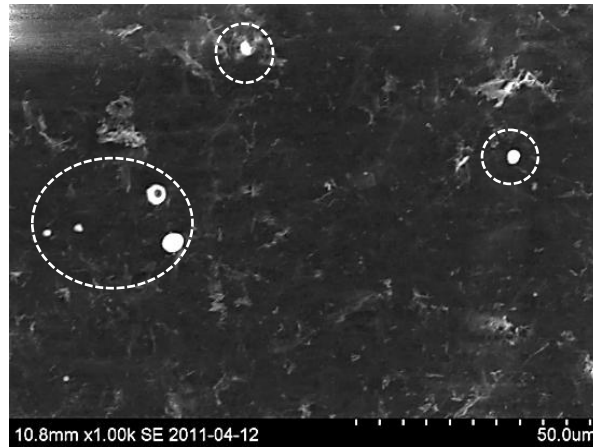


Figure 17: Typical SEM micrograph showing inclusions (white spots) dispersed over film filter matrix

4. RESULTS AND DISCUSSION

The results are divided into two main sections. The first section deals with the selection of electrolyte for electrolytic extraction. This selection depends on the properties and composition of inclusion in the steel samples. The second section investigates the change in the characteristics of inclusions as a function of time during secondary refining.

4.1 Selection of electrolyte for electrolytic extraction

To compare the effect of electrolytes on the properties of inclusions, sample 4 (S4) was selected for electrolytic extraction with 2% TEA and 10% AA electrolytes. SEM analysis of inclusions on the film filter was performed to investigate particle size distribution, morphology, shape and chemical composition. Finally, based on the effect of electrolytes on inclusion characteristics, the appropriate electrolyte is recommended for extraction experiments of other steel samples.

4.1.1 Particle size distribution

Cleanliness of steel is measured in terms of number of inclusions present in the steel product. The cleanliness increases with decreasing number of inclusions in steel. Equation 11 is used to calculate total number of inclusions per unit volume of steel.

$$N_v = \frac{n \cdot A_f}{A_{obs}} \cdot \frac{\rho}{\Delta w} \quad (0)$$

In above formula, N_v (inclusions/mm³) is the number of inclusions per unit volume of steel, n is the number of inclusions, A_f is the total area of the film filter, A_{obs} is the observed area on film filter, ρ is the density of steel (0.0078 g/mm³) and Δw is the dissolved weight of the metal. Figure 18 is showing the frequency of inclusions in steel in case of 2% TEA and 10% AA electrolytes. To investigate the size of inclusions which are being dissolved in 10% AA, the particle size distribution in case of the two electrolytes is shown in Figure 19.

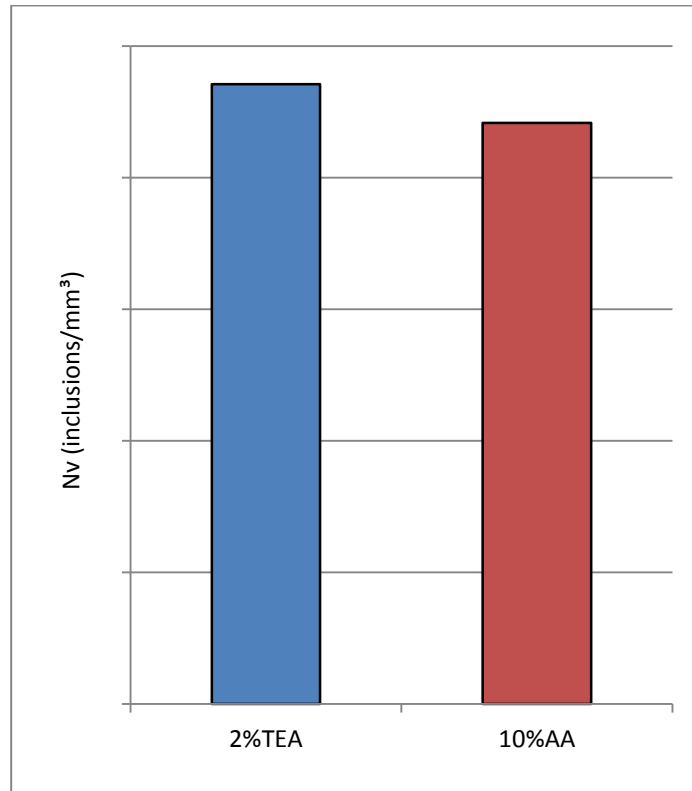


Figure 18: Total inclusion frequency in 2% TEA and 10% AA electrolytes

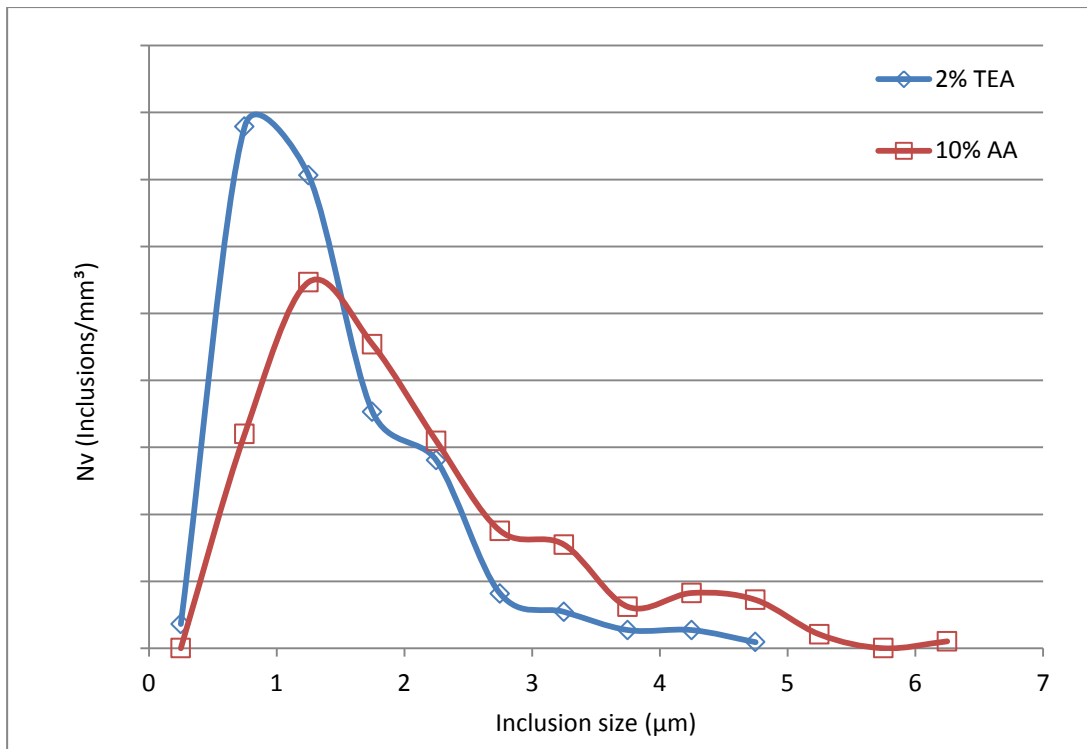


Figure 19: Particle size distribution in 2% TEA and 10% AA electrolytes

Theoretically, since the same sample is used in both cases, the inclusion frequency is expected to be similar if the electrolytes have similar effects on inclusions. The frequency in case of 10% AA is smaller (Figure 18) which suggests that some inclusions were either completely dissolved or reduced in size beyond measureable limit at 1000x magnification in SEM. This provides the first clue that 10% AA has negative effect on some inclusions.

Upon observing an area of 0.34mm² on film filter in both cases, ### inclusions were found in 2% TEA case while ### inclusions were seen in 10% AA case. Figure 19 shows that the number of inclusions in the size range 0.5 to 1.5 μm is higher in case of 2% TEA as compared to 10% AA. Beyond 1.5 μm, the size distribution for the two cases is almost same. This confirms the initial observation of reduction in total number of observed inclusions.

4.1.2 Shape and morphology comparison

The shape and morphology of inclusions are important characteristics which provide information about their state of existence in the steel melt. E.g. spherical shape suggests that the inclusions were in liquid state during solidification of steel matrix. For the comparison of electrolytes, the inclusions in sample S4 were classified into two shapes, namely spherical and non-spherical. Typical micrograph of each shape is presented in Figure 20.

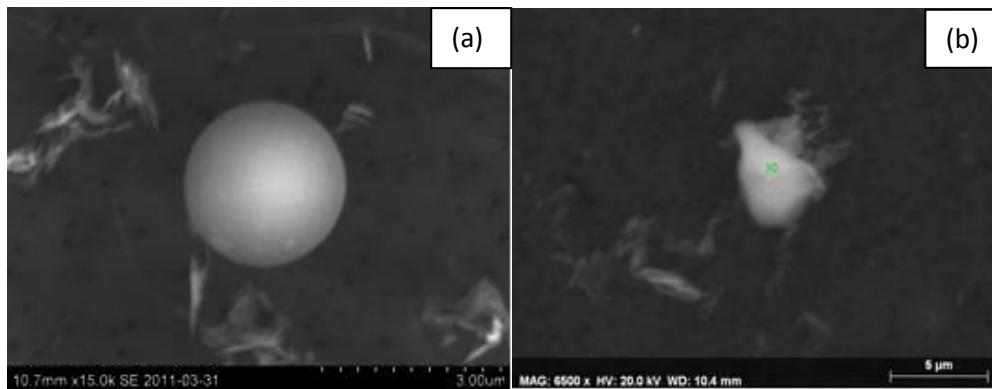


Figure 20: Typical (a) spherical and (b) non-spherical inclusion in S4

On the basis of morphology, the inclusions were classified into two categories; those with dissolved phases or holes and those without any holes. Typical inclusions with holes are shown in Figure 21.

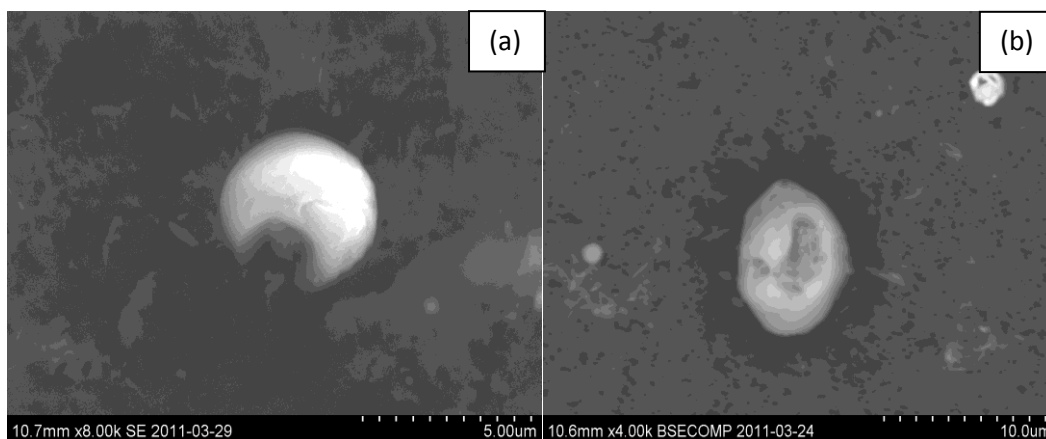


Figure 21: Typical holes in (a) spherical and (b) non spherical inclusions

For investigating the effect of 2% TEA and 10% AA electrolytes on the morphology of inclusions, the inclusions having holes in these electrolytes were compared. Presence of a hole indicates that some chemical phase in the inclusion might have dissolved in the electrolyte. Thus, the electrolyte having lesser number of inclusions with holes can be selected, as it is preserving the original composition and morphology of inclusions to higher extent. Table 2 shows the shape analysis data in case of 2% TEA and 10% AA. Figure 22 shows the percentage distribution of morphology of observed inclusions in the two electrolytes. It was investigated whether the effect of electrolytes depends on the shape of the particles. For this reason, spherical and non-spherical inclusions were analyzed separately.

Table 2: Inclusions analyzed for morphology in 2% TEA and 10% AA electrolytes

Electrolyte	Total inclusions	Spherical inclusions	Non-spherical inclusions
2%TEA	100	72	28
10% AA	103	86	17



Figure 22: Morphology distribution of inclusions in 2% TEA and 10% AA electrolytes

Figure 22 indicates that 10% AA electrolyte has a higher number of inclusions with holes. It was found that irrespective of the shape, 10% AA has more adverse effect on particle morphology which is reflected by more number of holes. Figure 22 shows that amount of inclusions with holes in 10% AA is approximately 2-4 times of those found in 2% TEA.

The distribution of inclusions with holes according to the size in case of 2% TEA and 10% AA electrolytes is shown in Figure 23. It indicates that 10% AA has more adverse effect on inclusions of all sizes compared to 2% TEA. The presence of holes seems to increase with inclusion size.

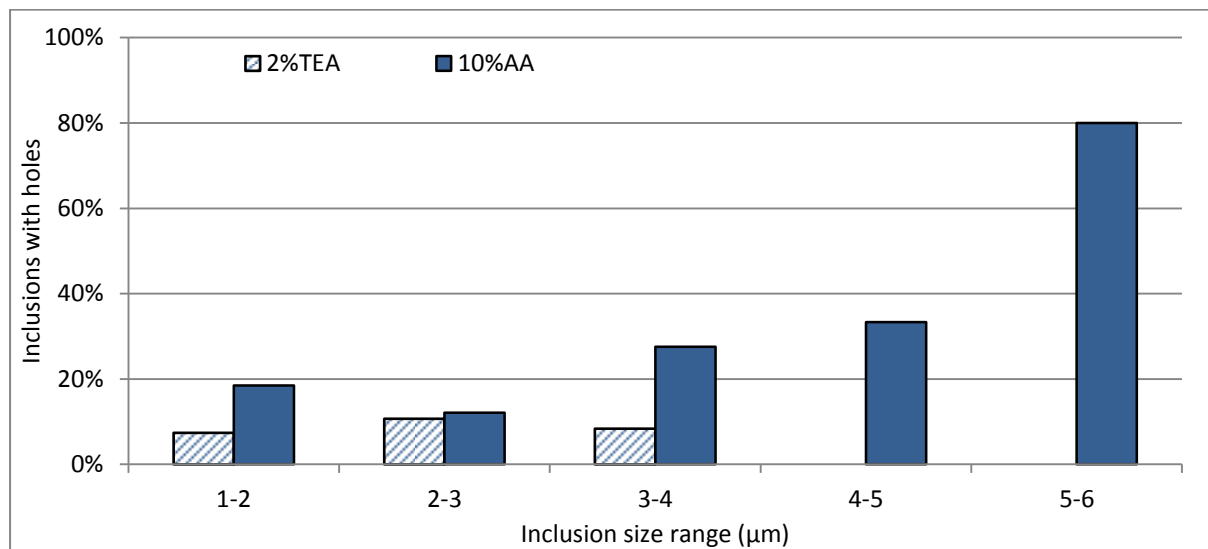


Figure 23: Number of inclusions with holes in each size range in 2%TEA and 10% AA electrolytes

Small size inclusions are solidified almost instantly while big inclusions take some time to solidify. This allows for separation of dissolved phases in larger inclusions. Thus, the presence of hole in larger inclusions gives a more convincing proof that some phases are preferentially dissolved. However, in the present study, only few inclusions were found in the size range 4-6 μm. It was already proved from particle size distribution that smaller particles were found to be dissolved in 10% AA. Thus, it can be concluded that 10% AA has adverse effects on inclusions of all sizes. Small size inclusions which may exist as a single

phase are uniformly dissolved while bigger size inclusions which may exist as combination of phases are partially dissolved, resulting in a hole. Therefore, the next section will deal with the investigation of the phases which are dissolved in 10% AA electrolyte.

4.1.3 Chemical composition of inclusions

From the previous discussion, it was already proved that 10% AA has 2-4 times higher number of inclusions with holes. Therefore, the present section emphasizes on the inclusions with holes in 10% AA and investigates the phase which is being dissolved by 10% AA.

Since three out of four samples are collected after the Ca addition to the melt, they were expected to contain a high portion of Ca aluminates. From the literature review, it is known that S present in the steel melt plays an important role in the formation of Ca aluminates. In the present study, the industrial samples were obtained from an ore based steel production route. Hence, they had considerable amount of S content. For this reason, it was necessary to consider the reactions and effects of S on the formation of Ca aluminates. Most commonly reported sulphides in steel are CaS and MnS. Among them, CaS is more stable than MnS at liquid steel temperature and forms at comparatively lower S content. For this reason, CaS is formed and exists in liquid steel while MnS is generally formed during the solidification when the rejected S from solidified steel increases the S content in remaining liquid.

Thermodynamically, Ca has higher affinity for O than S. Hence, when Ca is added to the melt, some of it reacts with dissolved oxygen to form CaO while the remaining Ca reacts with alumina inclusions to form aluminates. The aluminates formed initially are still not in the liquid phase. If the melt has high S content (>50 ppm), more added Ca reacts with S in the melt to form CaS and reduce dissolved S content. After the dissolved S is reduced below a certain level, more of the added Ca starts to react again with previously formed Ca aluminates to form liquid phases. This way, if the melt has high S content, a high amount of Ca is required for the Ca treatment to be successful. This may increase the cost of the operation and also lead to the formation of solid CaS (MP 2525°C) which may contribute to nozzle clogging like alumina inclusions.

Stoichiometric amount of CaS has S/Ca (wt%/wt%) ratio of 0.8. If the S/Ca in the inclusions is greater than 0.8, there is an excess of S after CaS formation. This excess S may form other sulphides like MnS during solidification. In this case, since the amount of Ca is less than stoichiometric amount required, the formation of CaS is controlled by Ca content. In the absence of CaO, alumina inclusions are not modified into liquid Ca aluminates. In the case of low S content (S/Ca<0.8), the excess Ca after CaS formation is available for the formation of Ca aluminates. In this case, the formation of CaS will be controlled by S content. For this reason, it is recommended to desulphurize the steel prior to Ca treatment. Liquid Ca aluminates also have high solubility of S and leads to the removal of S from the melt. However, this type of S removal is possible only when the melt already has a low S content, about 40 ppm.

Apart from Ca, no other elements were detected in the analysis of inclusions which can form sulphides. Hence, in the present study, the amount of CaS is considered to regulate the formation of Ca aluminates. This consideration helps to measure the amount of CaS together with Ca aluminates in the inclusions. The total Ca content measured by the composition analysis of inclusions was divided into Ca in CaS and Ca in aluminates.

$$Ca_A = Ca_M - Ca_S \quad (0)$$

In the above equation, Ca_A is the wt% Ca in Ca aluminates, Ca_M is the wt% Ca measured by SEM EDS analysis of the inclusions and Ca_S is the wt% Ca in CaS.

Each Ca aluminate phase in the binary phase diagram (Figure 6) has a certain Al/Ca (wt%/wt%) ratio. For calculating the Al/Ca ratio of aluminates, the formula used is given below:

$$\frac{Al}{Ca} = \frac{\text{measured Al (wt\%)}}{Ca_A \text{ (wt\%)}} \quad (0)$$

These ratios are presented in Table 3. In this way, different phase fields in binary phase diagram can be divided in terms of different Al/Ca ratio ranges. The inclusions analyzed in the present study were normalized for wt% Al, wt% Ca, wt% S and wt% O.

Table 3: Ratio of Al/Ca in various Ca aluminate phases

Aluminate phase	Al/Ca (wt%/wt%) ratio
$3\text{CaO} \cdot \text{Al}_2\text{O}_3$	0.45
$12\text{CaO} \cdot 7\text{Al}_2\text{O}_3$	0.787
$\text{CaO} \cdot \text{Al}_2\text{O}_3$	1.35
$\text{CaO} \cdot 2\text{Al}_2\text{O}_3$	2.7
$\text{CaO} \cdot 6\text{Al}_2\text{O}_3$	8.1

To investigate the phase which is being dissolved in 10% AA, the Al/Ca_A (wt%/wt%) of the inclusions with holes in 10% AA is plotted in Figure 24. An important point to note here is that the chemical composition of the inclusions with holes is analyzed only for the portion of the inclusion left after dissolution. Hence, it can be seen in Figure 24 that in the present study, C₃A, C₁₂A₇ and CA are the phases not affected by 10% AA.

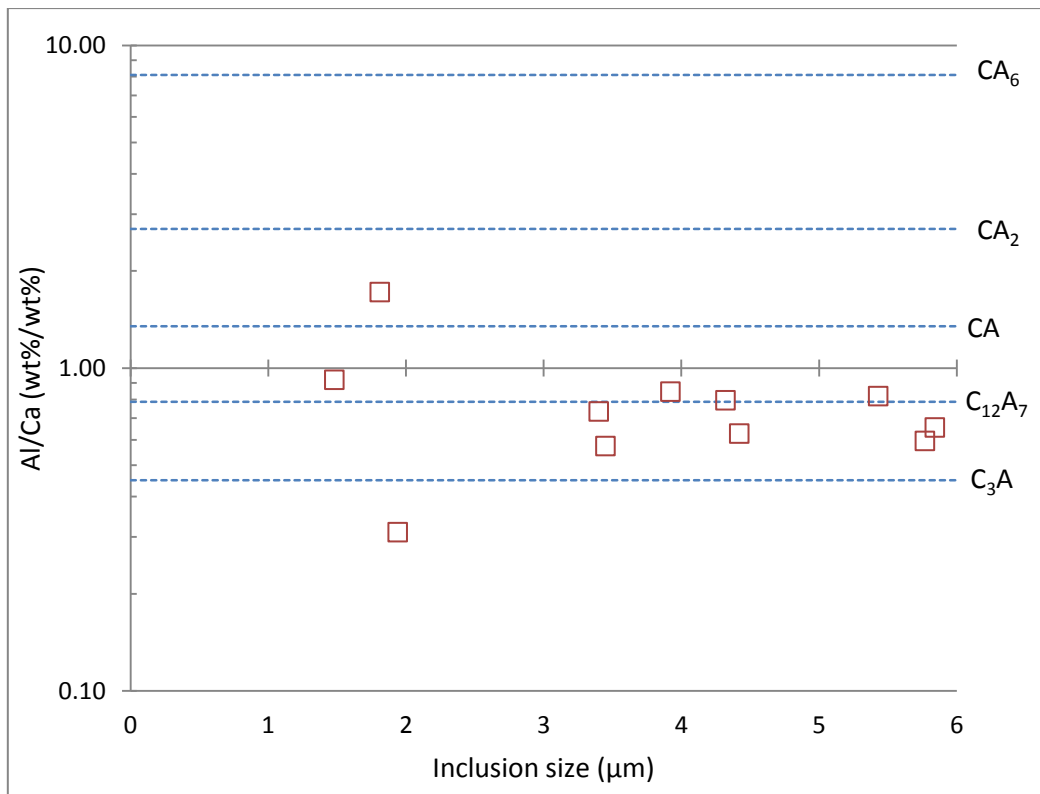
**Figure 24: Inclusions with holes in 10% AA**

Figure 25 shows the distribution of different phases in all analyzed inclusions (with and without hole) in 2% TEA and 10% AA electrolytes. Regarding CA_2 , CA and $C_{12}A_7$, the information is in agreement with Figure 24, i.e. 10% AA is preserving these phases. Looking more closely at the phase field $C_3A+C_{12}A_7$, it can be seen that 2% TEA is dissolving more of these phases compared to 10% AA. However, since the number of inclusions with holes in 2% TEA is lower (from morphology data), this dissolution is not of considerable importance and can be neglected in the present context.

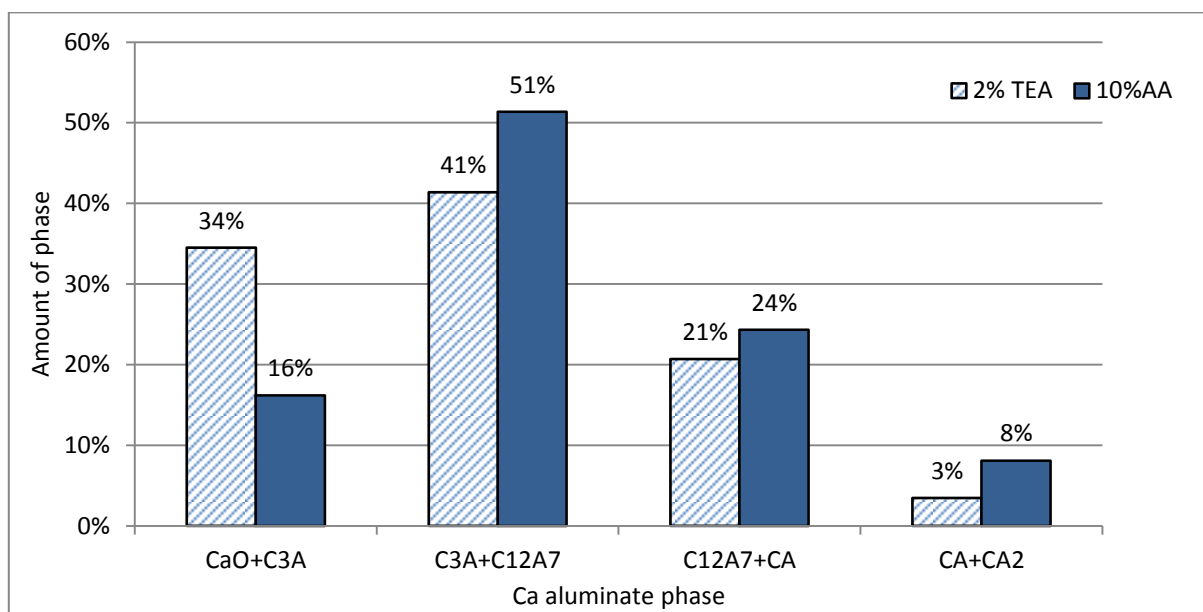


Figure 25: Amount of Ca aluminate phases in 2% TEA and 10% AA electrolytes

In case of $C+C_3A$ phase field (high Ca content phases), 10% AA has retained less than half the amount of these phases compared to 2% TEA. From the morphology results, the extent of dissolution in 10% AA was 2-4 times more than 2% TEA. Combining these two results, it can be concluded that 10% AA dissolves high Ca phases like pure CaO and C_3A . Hence, it is concluded that 2% TEA is a better electrolyte for the extraction of inclusions in case of Ca treated steels. For the inclusions consisting of mainly pure alumina, 10% AA electrolyte can be used effectively⁴⁴.

4.2 Changes in inclusion characteristics during secondary refining

In this section, the change in the inclusion characteristics during secondary refining of steel is discussed in terms of number of inclusions, their size distribution, shape, morphology and chemical composition. The analysis of these properties will help in attaining a better understanding of the transformation of inclusions during different stages of secondary refining of steel.

4.2.1 Particle size distribution

One way to improve the cleanliness of steel is to reduce the number of inclusions in the steel melt. Another way to improve the properties of steel is to modify the inclusions into acceptable composition, shape and morphology. Figure 26 shows the frequency of the total number of inclusions in different samples.

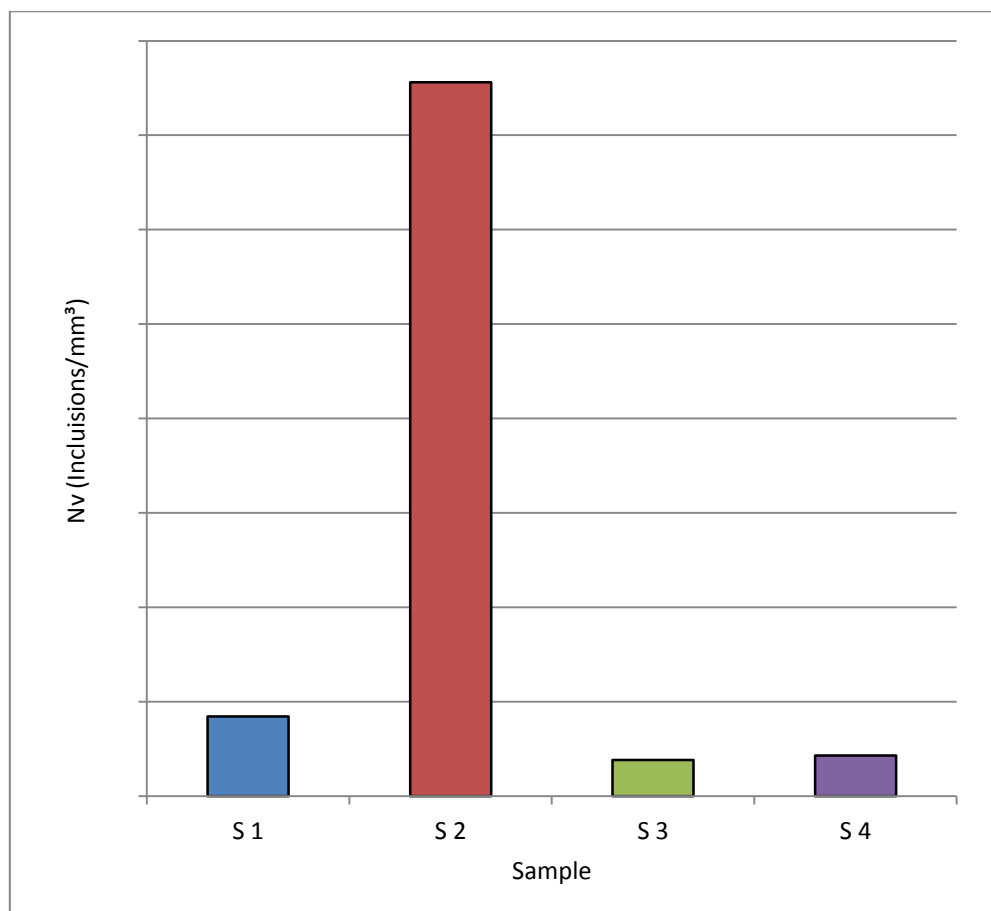


Figure 26: Total inclusion frequency in four samples

Figure 26 shows that after Ca addition, the number of inclusions have increased to a very high value. These inclusions could be a combination of older inclusions which were being modified into Ca aluminates and newer inclusions nucleated from Ca reacting with dissolved O in steel. The number of inclusions may also increase due to the dispersion of clustered alumina inclusions into many separate inclusions as a result of modification by Ca. This possibility is however discarded in the present case since very few clusters were observed in S1. Previous studies have suggested that clusters and big size inclusions are removed in about 15 min after deoxidation^{4,45}. This is in line with the observed results that very few clusters were observed in S1 which was sampled about 30 minutes after deoxidation. Hence, the dispersion of clusters does not contribute much to the rise of inclusions in S2.

There is a sharp decrease in the number of inclusions from S2 to S3. This decrease can be explained by looking into the mechanism of growth and separation of inclusions. After ladle treatment at CAS-OB station, the ladle is transported to the casting station. This is followed by the teeming of liquid steel from the ladle into the tundish. This time gap (about 50-60 minutes) between the sampling of S2 and S3 is expected to be sufficient for the inclusions to grow and coalesce together. This phenomenon explains the formation of larger inclusions at the expense of smaller ones, thus reducing their total number in the melt. More importantly, these bigger inclusions are expected to be easily separated into the slag compared to the small ones on account of larger buoyant force acting on them. Thus, at the time of starting the casting operation, a large portion of inclusions might have already separated from the melt. S3 and S4 show similar behaviour which indicates that the steel in the tundish had uniform number of inclusions during the whole casting operation.

For a deeper insight into the change in the number of inclusions, the particle size distribution in different samples is plotted in Figure 27. S1 was expected to contain mainly the alumina inclusions which are reported to form clusters. In contrast, S1 does not show many large size clusters. This may be accounted to the appreciable time difference of more than 30 minutes between addition of Al to the melt and sampling of S1. During this time, the big size clusters (> about 12 μ m) might have separated from the melt, hence the steel sample from the melt did not have many clusters. It can be seen that the variation in the frequency of inclusions in different samples is mainly for small inclusions of about 1 μ m. S2 curve in Figure 27 shows a large number of only small size inclusions. This confirms the

assumption that the increase in the number of inclusions is largely due to the nucleation of small inclusions after Ca addition. S3 and S4 show almost similar distribution of the inclusions which again confirms that the steel in the tundish had uniform distribution of inclusions during continuous casting.

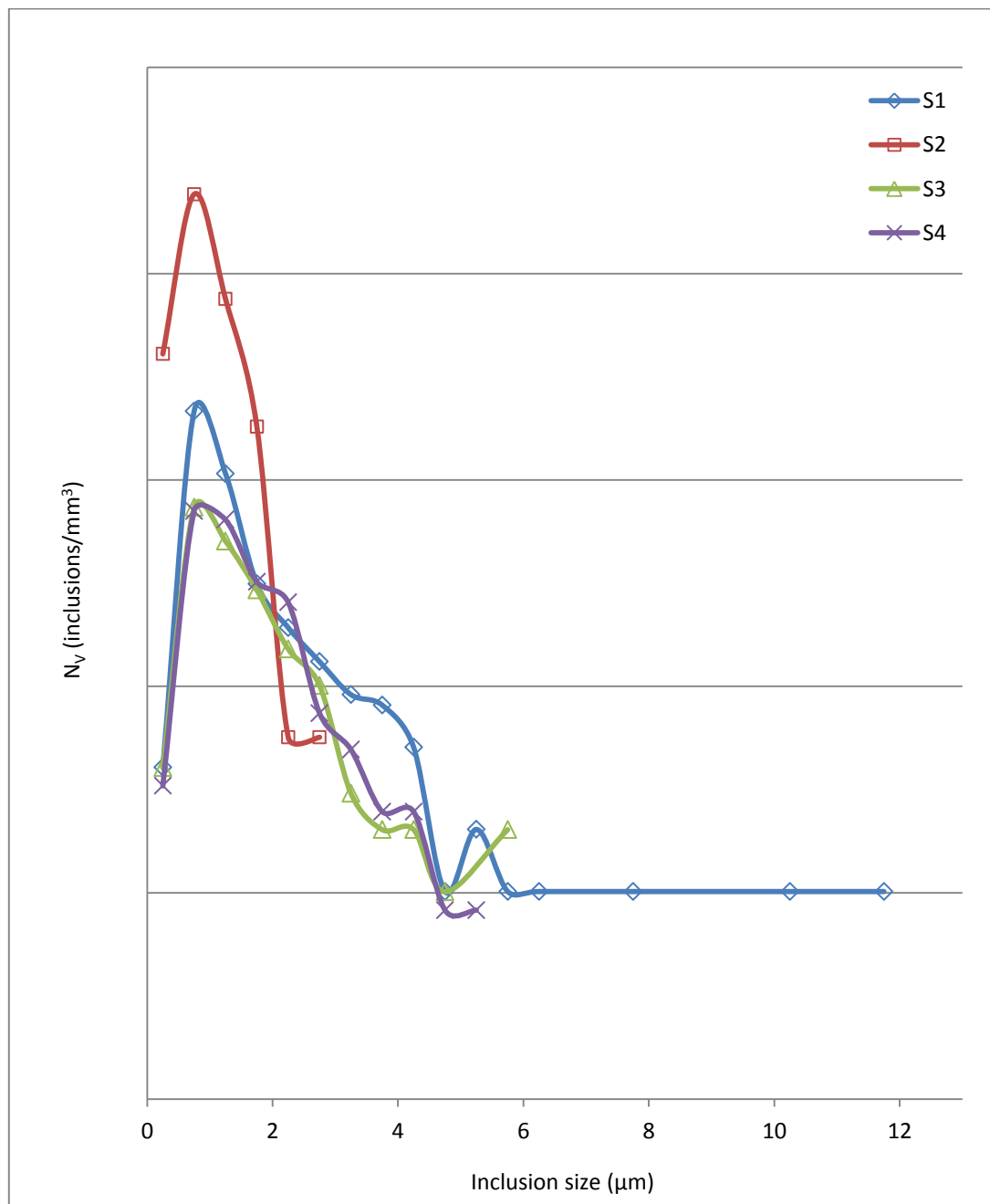

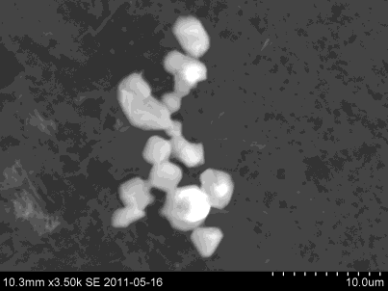
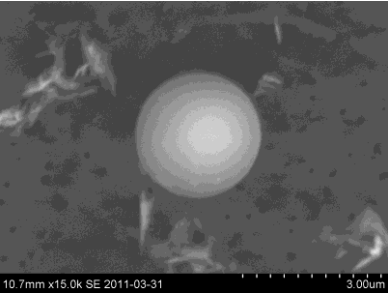



Figure 27: Particle size distribution in four samples

4.2.2 Morphology

Ca addition modifies the alumina inclusions into Ca aluminates. Certain Ca aluminates have lower melting point than the solidification temperature of steel. These Ca aluminates are expected to have spherical shape, since they were liquid at casting temperature. Some typical shapes and morphologies of inclusions are presented in Table 4.

Table 4: Typical inclusion types and their properties in investigated samples

Inclusion Micrograph	Sample no.	Size (μm)	Contents (wt %)	Compound
	1	1-2	Al (37-48)	Alumina (Hexagonal geometry suggests Corundum)
	1	5-22	Al (40-49)	Alumina clusters
	2, 3, 4	0.7-6	Al (1-14) Ca (28-40) S (15-22)	Ca aluminates (liquid at casting temperature)
	1, 2, 3, 4	0.8-4	Al (2-15) Ca (0.5-40) S (10-40)	Solid Ca aluminate phases and sulphides

The efficiency of Ca treatment can be estimated by the amount of spherical inclusions formed after Ca addition. These spherical inclusions are believed to represent the liquid zone in CaO-Al₂O₃ binary phase diagram. Figure 28(a) shows a sharp increase in the number of spherical inclusions after Ca addition. On an average, Ca treatment has shown to retain 67-78% spherical inclusions. This reflects that these inclusions were present in liquid state during the casting and solidification of steel. Chris¹⁴ has reported that clogging is avoided if the inclusions contain more than 50 % liquid phases in the liquid steel. Hence, it can be said that nozzle clogging can be at least delayed to some extent by the Ca treatment of steel. These Ca aluminates which end up in the final cast product are more acceptable than pure alumina since they are less hard and expected to bend easily with the steel matrix during the rolling operation. The conversion of MnS into CaS is also beneficial since hydrogen gets entrapped in the elongated MnS, thereby increasing the risk of hydrogen induced cracking (HIC). CaS being harder and almost undeformable, prevents these risks^{46,47}.

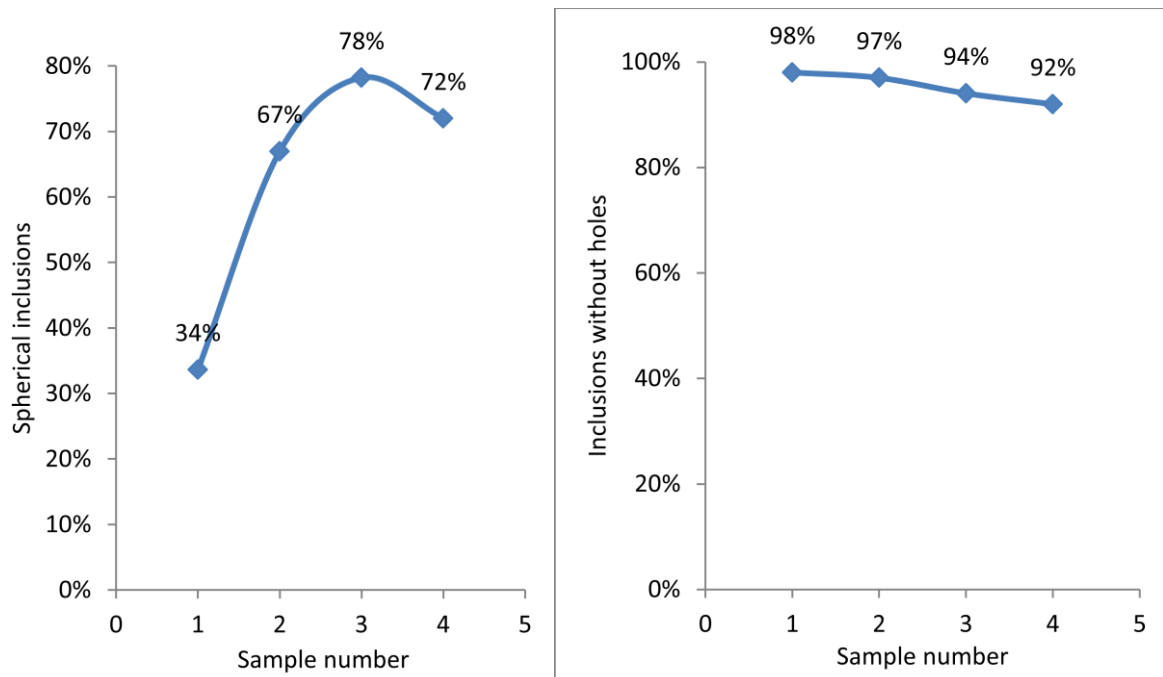


Figure 28: Change in (a) shape and (b) morphology of inclusions in different samples

Figure 28(b) shows that more than 90% of the inclusions were without holes after electrolytic extraction. This confirms that selecting the appropriate electrolyte initially in the project and using it for electrolytic extraction was a necessary step in inclusion characterization. If the selection of the appropriate electrolyte would not have been performed, inclusions from S2 would have been worst affected as they are largely composed of high Ca phases.

4.2.3 Chemical composition of inclusions

The compositional analysis of the inclusions from different stages of secondary refining gives an idea of the phase transformation in the inclusions. The inclusions in steel samples were found to contain small amount of Mg (about 1-2 wt%). Tshilombo⁴⁸ also found similar quantities of MgO in the micro-inclusions after Ca treatment. Potential sources of Mg include refractory lining, slag and aluminium added for deoxidation which contains about 0.5wt% Mg⁴.

For investigating the shift in chemical composition, the inclusions are depicted in CaS, CaO, Al₂O₃ ternary diagrams in Figure 29. The wt% of these compounds in the inclusions was calculated according to the method employed in section 4.1.3. It is important to note that these diagrams are plotted on the basis of normalized wt% of these three components in each inclusion. It can be seen that the inclusions with almost same composition appear as overlapping points in the diagrams. After Ca addition, the composition is seen to be shifting from pure Al₂O₃ to the CaO-CaS region. Gradually some Al₂O₃ reappears in S3 and S4 which is reflected by the presence of some inclusions near the center of the triangle.

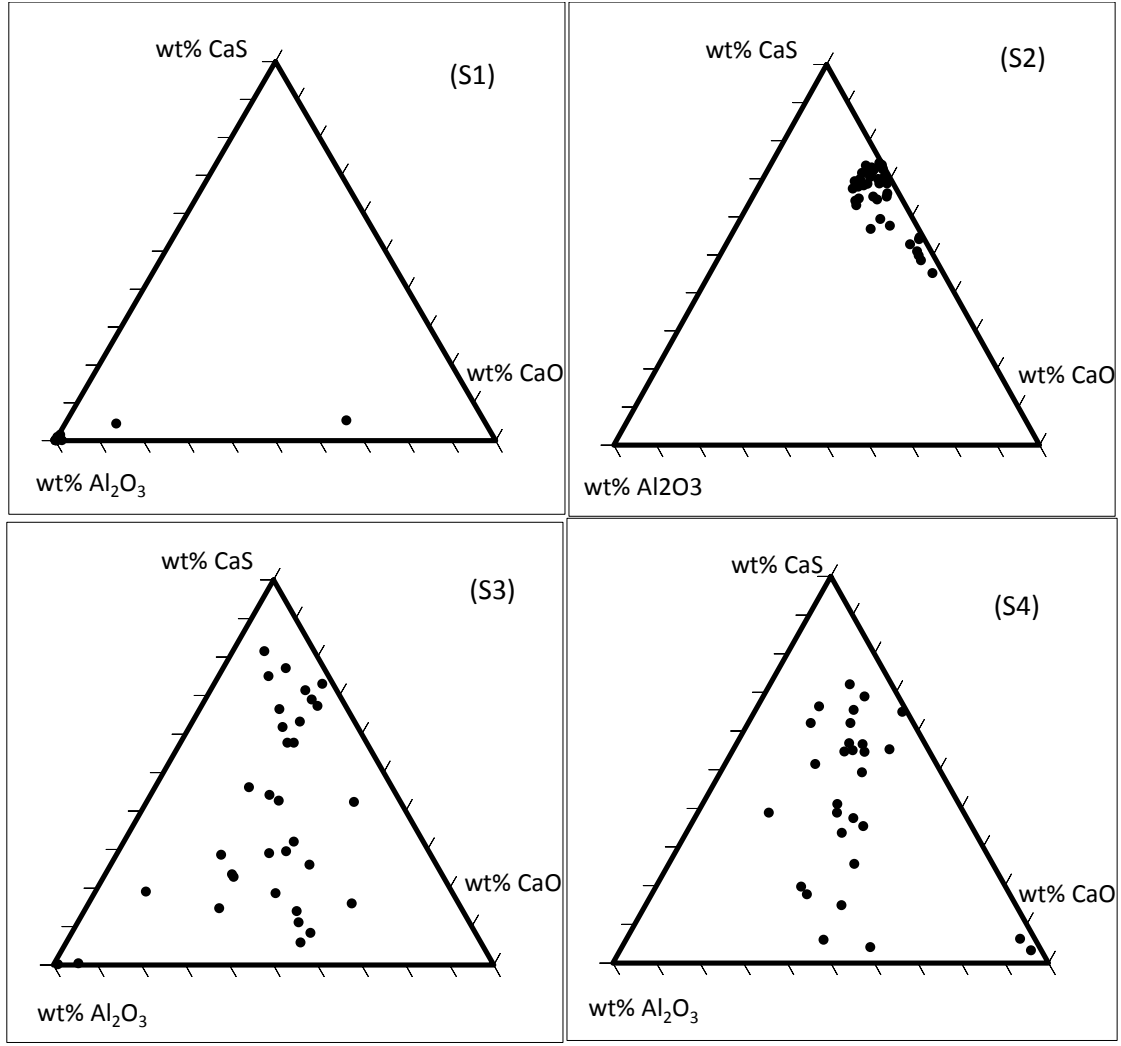


Figure 29: Composition of inclusions in steel samples

In order to study the effect of Ca treatment, it is important to know the amount and composition of Ca aluminates in inclusions. To calculate the wt% of Ca aluminate in inclusions, let the chemical formula of Ca aluminate be $P(\text{CaO}) \cdot Q(\text{Al}_2\text{O}_3)$. Let the inclusion have R moles of this compound. So, the inclusion contains RP moles of CaO and RQ moles of Al_2O_3 .

Replacing 'RP' by single variable 'X' and 'RQ' by 'Y':

$$\text{wt\% Ca (Ca}_A\text{)} = 40 \cdot X \quad (1)$$

Calculating Al/Ca (wt%/wt%) ratio,

$$\frac{Al}{Ca_A} = \frac{Y \cdot (27.2)}{wt\% Ca} \quad (1)$$

$$Y = \frac{wt\% Ca}{54} \cdot \frac{Al}{Ca_A} ratio$$

Mass (wt%) of Ca aluminate in inclusion

$$\begin{aligned} &= X \cdot (40 + 16) + Y \cdot (27.2 + 16.3) \\ &= 56 \cdot X + 102 \cdot Y \end{aligned} \quad (1)$$

$$= \frac{7}{5} \cdot Ca_A + \frac{51}{27} \cdot Ca_A \frac{Al}{Ca_A} ratio$$

$$= Ca_A \left(\frac{7}{5} + \frac{17}{9} \cdot \frac{Al}{Ca_A} ratio \right)$$

S/Ca<0.8 (from section 4.1.3) and Al/Ca ratio smaller than about 10 (from Figure 6) are considered the necessary conditions in the present calculations for the formation of Ca aluminate. In cases where these conditions are fulfilled, Al is considered to exist entirely in Ca aluminate. If Ca aluminate is not formed, Al is considered to exist as pure alumina. However, Ca is considered to be distributed in CaS and Ca aluminate. In this way, the wt% of CaS, Ca aluminate and alumina is calculated for the inclusions. For classification purpose, the inclusions were assigned a category if they had >70 wt% of that component. If an inclusion had 30-70wt% of two different components, it was regarded as a combination of constituent components. In this way, all 40 inclusions in each sample were categorized in Figure 30.

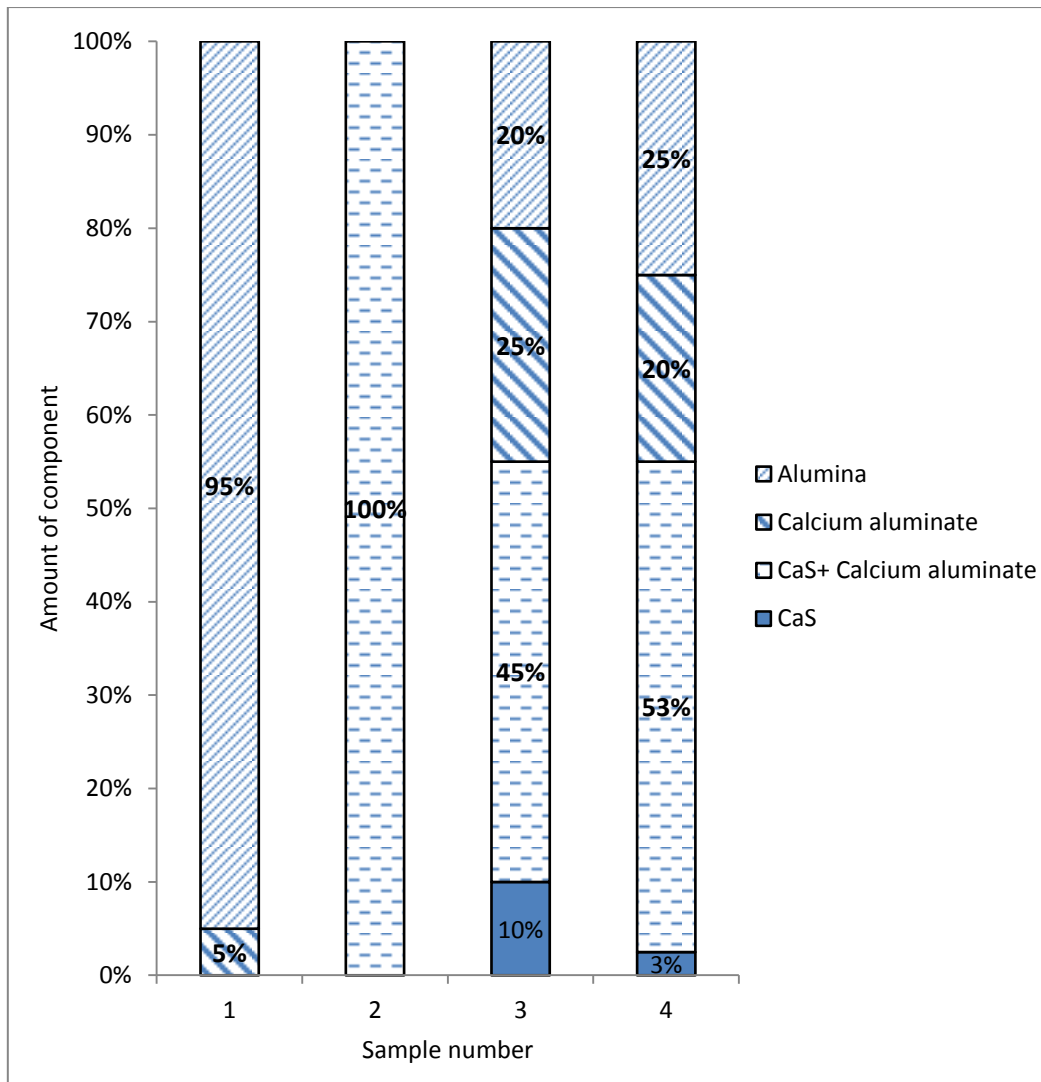


Figure 30: Distribution of components in different samples

Most of the inclusions in sample S1 were pure alumina which is in line with the expected results since this sample was collected after Al deoxidation and before Ca addition. Sample S2, collected after Ca addition, shows large number of Ca aluminates-CaS type inclusions. Lis²² found similar composition of the inclusions after Ca treatment. This behavior might be attributed to the high affinity of Ca towards O and S. It also shows that Ca aluminates have high S solubility. In this way, the dissolved S from the melt goes into the inclusions which are subsequently separated from the melt to some extent²². As the dissolved S content of steel is reduced, S is prevented from precipitating at grain boundaries. This decreases the risks of

corrosion and other defects in steel²². The Ca aluminate inclusions which end up in the final steel product are also less harmful compared to pure alumina inclusions.

In sample S3, some pure Ca aluminates and CaS can be seen. Also some alumina reappears in the inclusions. The possible sources of alumina at this stage include slag entrapment, refractory linings and reoxidation phenomena during the time of ladle transport to casting station and teeming operation. The reappearance of alumina in the tundish steel has also been reported by Rampersadh and Pistorius from their studies⁴⁹. It is important to remember that S3 is taken at 20 minutes after the start of continuous casting. The properties of inclusions present in steel melt at this stage are crucial in deciding the ease of casting operation. Also, these inclusions will end up in the final cast product. The presence of 70% inclusions in S3 as Ca aluminate indicates the success of Ca treatment operation. Similar properties of inclusions are also seen in S4. Hence, it can be said that the distribution and composition of the inclusions in the tundish melt was same throughout the casting operation.

Based on the different values of Al/Ca_A in the inclusions, they can be classified into different Ca aluminate phases according to Table 3. This classification is shown in Figure 31 which indicates whether the aim of forming inclusions in the liquid zone of binary phase diagram is successful. It can be seen that after Ca addition there is a large increase in number of Ca aluminates. Sample S3 contains 70% of the inclusions as Ca aluminates, almost all of which belong to the liquid zone²². This behavior is continued in S4 which confirms that the Ca treatment has been successful in achieving the composition corresponding to the liquid Ca aluminates.

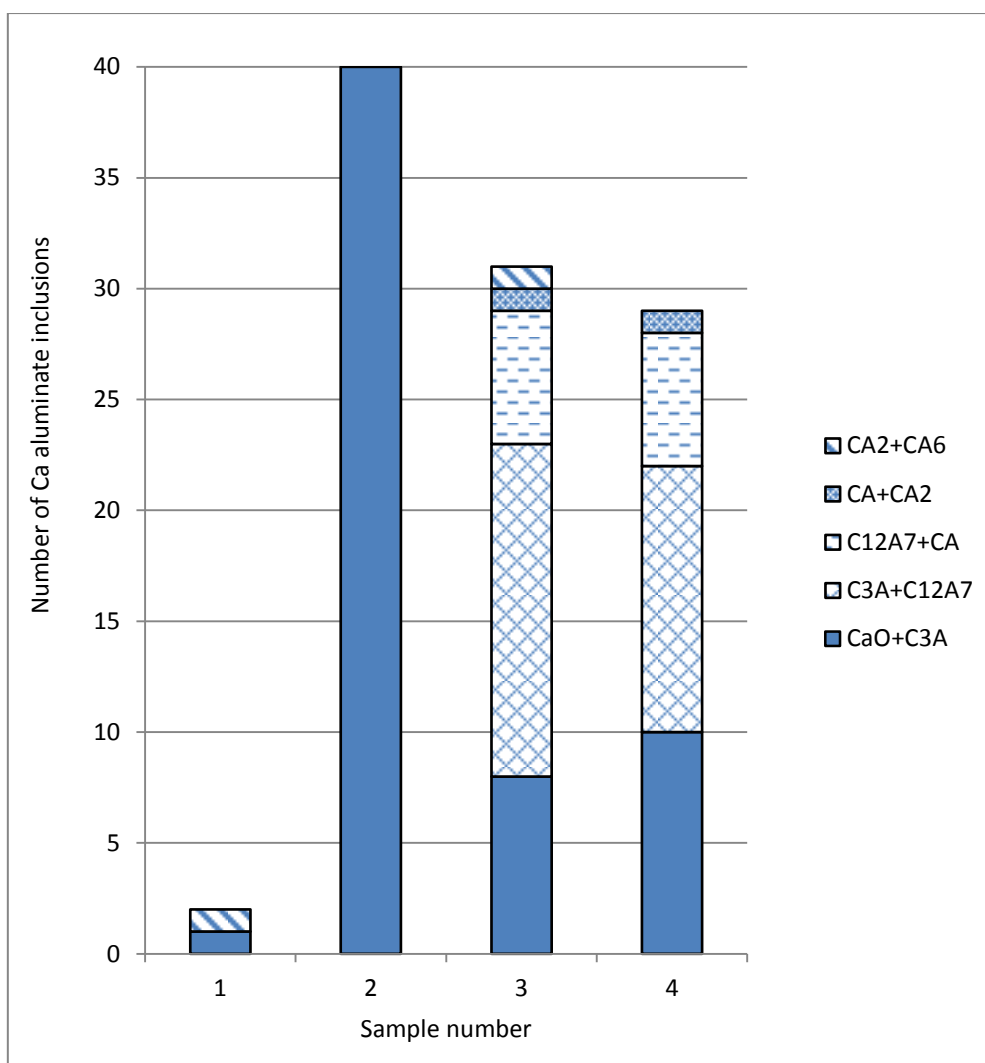


Figure 31: Distribution of different Ca aluminates in steel samples

5. CONCLUSIONS

Selection of electrolyte was performed for the electrolytic extraction of inclusions in steel samples. Conclusions in this part of the study are as follows:

- The electrolytic extraction can be successfully utilized as a method for the 3D study of the inclusion characteristics.
- 2% TEA was found to be a better electrolyte than 10% AA for the electrolytic extraction of inclusions having a high Ca content.

Changes in inclusion characteristics with time during secondary refining of steel were investigated. Based on changes in number of inclusions, their shape, morphology and chemical composition, the conclusions are as follows:

- On Ca addition to liquid steel, the number of small size (about 1 μm) CaO-CaS inclusions first increase to a very high value. The reaction between Ca and dissolved O would result in the nucleation of new inclusions along with the existing inclusions which were modified into Ca aluminates. This increase was followed by a large decrease in the number of inclusions which may have been caused by the growth and subsequent separation of the inclusions into the slag phase.
- Some alumina reappears in the melt in tundish. This may be caused due to the reoxidation during transport to the casting station and teeming process. Other possible sources of alumina include refractory lining and slag entrapment.
- The properties of inclusions at the start and end of continuous casting were found to be similar. This confirms that the liquid steel in the tundish had uniform distribution and composition of inclusions during the casting operation.
- Ca treatment resulted in about 67-78% of spherical inclusions which confirms the success of Ca treatment. The spherical shape suggests that these inclusions were in the liquid state during casting.
- Ca treatment of LCAK steel produces Ca aluminates shifting from CaO towards the liquid zone, i.e. inclusions consisting of CaO, $3\text{CaO}\cdot\text{Al}_2\text{O}_3$ and $12\text{CaO}\cdot 7\text{Al}_2\text{O}_3$. Hence, the shape and morphology results are complimented by the chemical composition results that the spherical inclusions correspond to the liquid zone in CaO- Al_2O_3 system.

6. FUTURE WORK

- Although the single heat results have shown successful application of Ca treatment process, more heats (set of samples) can be analyzed to confirm the consistency of results.
- A higher number of inclusions can be considered and a higher magnification can be used for the analysis of particle size distribution, shape, morphology and chemical composition of the inclusions to improve the statistical accuracy.
- Some more samples can be collected for a closer look of the phase transformation of inclusions during ladle transportation between the CAS-OB station and the continuous casting station.

7. REFERENCES

¹ www.ssab.com, 2011-06-11

² M. Andersson, T. Sjökvist and P. Jönsson: *Ladle metallurgy*; Chapter 4, Printed in Sweden 2006

³ B. Deo and R. Boom: *Fundamentals of steelmaking metallurgy*; Chapter 17

⁴ R. Dekkers, B. Blanpain, P. Wollants, F. Haers, C. Vercruyssen and B. Gommers: *Non-metallic inclusions in Aluminium killed steels*; Ironmaking and Steelmaking, Vol. 29 (6), 2002

⁵ L. Nilsson, K. Andersson and K. Lindquist: *The CAS-OB process in the steelshop at SSAB Tunnplåt AB, Luleå Works*; Scandinavian journal of metallurgy, ISSN 0371-0459; 1996 Vol. 25, pp 73-79

⁶ <http://www.keytometals.com/articles/art62.htm>, 2011-06-12

⁷ www.steeluniversity.org, 2011-05-14

⁸ R. Monroe: *Porosity in castings*; AFS Transactions 2005, American Foundry society, Schaumburg, IL USA, Paper 05-245 (04)

⁹ K. Torssell, *Jernkontorets Annaler* 151, 1967, pp 890-949

¹⁰ B. Deo and R. Boom: *Fundamentals of Steelmaking metallurgy*; Chapter 16 (Thermodynamic fundamentals)

¹¹ K. G. Rackers and B. G. Thomas: *Clogging in continuous casting nozzles*; 78th Steelmaking conference proceedings, Nashville, TN, April 2, 1995, Iron and Steel society, Warrendale, PA, Vol. 78, pp 723-734

¹² L. Zhang and B. G. Thomas: *Inclusions in continuous casting of steel*; XXIV National Steelmaking Symposium, Morelia, Mich, Mexico, 26-28 Nov.2003, pp 138-183

¹³ J. C. S. Pires and A. Garcia: *Modification of oxide inclusions present in aluminium-killed low carbon steel by addition of calcium*; REM: R. Esc. Minas, Ouro preto, 57(3), 2004, pp 183-189

¹⁴ P. Chris: *Magnesium- Origin and role in calcium treated inclusions*; Extraction and Processing division; International symposium, California, 2006 pp 373

¹⁵ Z. J. Han, L. Liu, M. Lind and L. Hollapa; *Mechanism and kinetics of transformation of alumina inclusions by calcium treatment*, Acta Metall. Sin. Engl. Lett. 19, 2006, pp 1

¹⁶ F. Yuan, X. Wang and X. Yang; *Influence of calcium content on solid ratio of inclusions in Ca-treated liquid steel*; J Univ. Sci. Tech. Beijing, 13, 2006, pp 486

-
- ¹⁷ M. Andersson: *A study of tundish nozzle blockage during casting of aluminium deoxidized steel*; (Chapter 19)
- ¹⁸ R. Dekkers: *Doctoral Thesis*; Katholieke Universiteit Leuven, Faculteit Wetenschappen, Department of Geografie-Geologi, *Chapter 10: Improvement of steel cleanliness*, Belgium, June 2002
- ¹⁹ A. L. Kundu, K. M. Gupt and P. K. Rao: *Morphology of non-metallic inclusions using aluminium and calcium-silicon alloy in melt*; metallurgical transactions B, Vol. 20B, Oct 1989
- ²⁰ T. Engh: *Principles of metal refining*, Chapter 15
- ²¹ O. Wijk: *Inclusion Engineering*; Chapter 18
- ²² L. Teresa: *Modification of oxygen and sulphur inclusions in steel by calcium treatment*; Metallurgia 48(2009)2, Faculty of Metallurgy, Aleja Narodnih heroja 3, Sisak, 44103, Croatia pp 95-98
- ²³ K. Larsen and R. J. Fruehan: *ISS Transactions*, V.12, 1991, pp 125-132
- ²⁴ H. Gaye, M. Gatellier, M. Nadiff and P. V. Riboud: *Revue de Metallurgie – CIT*, 84 (1987)11, pp 759-771
- ²⁵ M. Lind and L. Holappa: *Transformation of alumina inclusions by calcium treatment*; Metallurgical and materials transactions B, Vol. 41B, April 2010
- ²⁶ R. Kiessling: *Non-metallic inclusions in steel*; (chapter 20)
- ²⁷ Y. Guozhu, P. Johnsson and T. Lund: *Thermodynamics and Kinetics of the modification of Al_2O_3 inclusions*; ISIJ Int., 36 Supplement, 1996, pp 105-108
- ²⁸ J. Janke, Z. Ma and P. Valentin, et al: *Improvement of castability and quality of continuously cast steel*; ISIJ Int., 40 (1), 2000, pp 31-39
- ²⁹ E. A. Chichkarev: *Conditions for Non-metallic inclusion formation in steel deoxidized with Aluminium and calcium*; Metallurgist, Vol. 53, 2009, pp 11-12
- ³⁰ N. Bannenbergh: *Steelmaking Conference proceedings*, 1995, pp 457-463
- ³¹ E. T. Turkdogan: *Deoxidation of Steel*; JISI 1972, pp 21-36
- ³² S. Linder; *Hydrodynamics and collisions of small particles in a turbulence metallic melt with special reference to deoxidation of steel*; Scand. J. Metallurgy, Vol. 3, 1974, pp 137-150
- ³³ M. Suzuki, R. Yamaguchi, K. Murakami and M. Nakada; *Inclusion particle growth during solidification of stainless steel*; ISIJ Inter. Vol. 41(3), 2001, pp 147-256

-
- ³⁴ K. Nogi; *Wetting phenomena in materials processing*; Tetsu-to-Hagane, Vol. 84(1), 1998, pp 1-6
- ³⁵ M. Fernandes, J. C. Pires, N. Cheung and A. Garcia: *Influence of refining time on non-metallic inclusions in a low-carbon, silicon killed steel*; Materials characterization 51 (2003), pp 301-308
- ³⁶ R. Rastogi and A. W. Cramb; *Inclusion formation and agglomeration in Aluminum killed steels*; Steelmaking conference proceedings, Vol. 84, ISS, Warrendael, (Baltimore, Maryland, USA) 2011, pp 789-829
- ³⁷ N. Verma, P. C. Pistorius and R. J. Fruehan: *Modification of spinel inclusions by calcium in liquid steel*; AIST transactions Vol. 7 No.1, July 2010
- ³⁸ G. Wranglen: *Pitting and Sulphide inclusions in steel*; Corrosion science Vol.14 (5), 1974, pp 331-349
- ³⁹ C. Lincourt and M. Krishnadev: *Effect of inclusion morphology on the fracture toughness of high strength steels*; Laval University, Dept. of Mining, Metallurgical and Material Engineering, Quebec, Canada, G1V 0A6, Hydro-Quebec Research Institute, 1800 Blvd Lionel-Boulet, Varennes, Quebec, Canada J3X 1S1
- ⁴⁰ S. Kimura, K. Nakajima and S. Mizoguchi: *Behavior of alumina-magnesia complex inclusions and magnesia inclusions on the surface of molten low-carbon steels*; metallurgical and materials transactions B, Vol.32B, Feb 2001
- ⁴¹ H. Doostmohammadi , A. Karasev and P. G. Jönsson: *A comparison of a two-dimensional and a three-dimensional method for inclusion determination in tool steel*; Steel research international, Vol. 81, Issue 5, May 2010, pp 398-406
- ⁴² <http://mee-inc.com/esca.html>, 2011-05-10
- ⁴³ M. Suazo: *Application of EE for 3D investigation of inclusions in Austenitic stainless steel*; Master thesis, Royal Institute of Technology, Stockholm, 2010
- ⁴⁴ R. Inoue, T. Ariyama and H. Suito: *Extraction and evaluation of inclusion particles in steel*; Asia steel international conference 2009, S11-16, pp 1-9, May 24-27, 2009, Korean institute of metals and materials
- ⁴⁵ M. Jefford, G. Betka, S. McIntosh and L. D. Way: *Proc. 3rd Int. Cong. On 'Oxygen steelmaking'*, Oct-Nov 2000, Birmingham, UK, Iron and steel division, The institute of materials, pp 307-317
- ⁴⁶ C. E. Cicutti, J. Madias and J. C. Gonzales: *Control of microinclusions in calcium treated aluminium killed steels*; Ironmaking and steelmaking, 1997, Vol 24, No.2

⁴⁷C. Blais, G. L'Espérance, H. LeHuy and C. Forget: *Development of an integrated method for fully characterizing multiphase inclusions and its application to calcium-treated steels*; Materials characterization 38 (1997), pp 25-37

⁴⁸ K. Tshilombo: Determination of inclusions in liquid steel after calcium treatment; International journal of minerals, metallurgy and materials, Vol. 17, No.1, Feb, 2010, pp28

⁴⁹ R. Rampersadh and P. C. Pistorius: *Reoxidation and castability of aluminium killed steels*; Journal of the south African institute of mining and metallurgy, Vol. 106, April 2006